

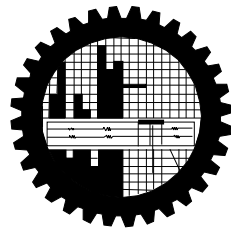
STUDY OF THE EFFECT OF MESH QUALITY ON STRESS CONCENTRATION FACTOR OF PLATES WITH HOLES USING FINITE ELEMENT ANALYSIS

Master of Philosophy
in
Mathematics

Sharaban Thohura

Student No.: 100709007 P

Session: October-2007



Department of Mathematics
Bangladesh University of Engineering & Technology
Dhaka-1000, Bangladesh.
November, 2012

STUDY OF THE EFFECT OF MESH QUALITY ON STRESS CONCENTRATION FACTOR OF PLATES WITH HOLES USING FINITE ELEMENT ANALYSIS

A dissertation submitted to the
Department of Mathematics
Bangladesh University of Engineering & Technology
In partial fulfillment of the requirement for the award of the degree of

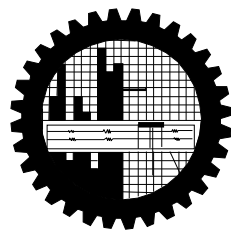
**Master of Philosophy
in
Mathematics**

Submitted by

Sharaban Thohura

Student No.: 100709007 P

Session: October-2007



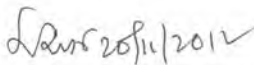
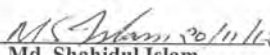
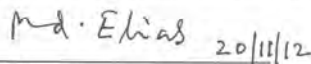
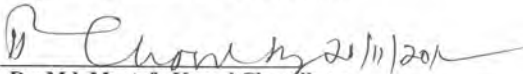
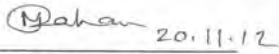

Department of Mathematics
Bangladesh University of Engineering & Technology
Dhaka-1000, Bangladesh.
November, 2012

The thesis titled
**Study of the effect of mesh quality on stress concentration factor of
plates with holes using finite element analysis**

Submitted by
Sharaban Thobura

Student No. 100709007 P, Session: October-2007, a part time student of M. Phil.
(Mathematics) has been accepted as satisfactory in partial fulfillment for the degree of
Master of Philosophy in Mathematics
November 2012

BOARD OF EXAMINERS

1. 
Dr. Md. Manirul Alam Sarker
Professor
Dept. of Mathematics, BUET, Dhaka. Chairman
(Supervisor)
2. 
Dr. Md. Shahidul Islam
Associate Professor
Dept. of Naval Architecture and Marine Engg., BUET, Dhaka. Member
(Co-Supervisor)
3. 
Head
Dept. of Mathematics, BUET, Dhaka. Member
(Ex-Officio)
4. 
Dr. Md. Mustafa Kamal Chowdhury
Professor
Dept. of Mathematics, BUET, Dhaka. Member
5. 
Dr. Md. Mustafizur Rahman
Professor
Dept. of Mathematics, BUET, Dhaka. Member
6. 
Dr. Amulya Chandra Mandal
Professor
Dept. of Mathematics, University of Dhaka, Dhaka. Member
(External)

DEDICATION

This work is dedicated to my beloved daughter

Nadhrahtan Nayem Numaira

Contents	I
Abstract	IV
Declaration	V
Acknowledgement	VI
Nomenclature	VII
List of Tables	IX
List of Figures	X
Chapter 1	1
Introduction and Literature Review	1
1.1 Introduction	1
1.2 Review of the previous work	7
1.3 Objectives of this thesis	9
1.4 Outline of Methodology	10
1.5 Thesis Framework	11
Chapter 2	13
Basics of Finite Element Method	13
2.1 What is The Finite Element Method (FEM)	13
2.2 How/Why should we study the method	14
2.3 Fundamentals of Finite Element Method	15
2.4 Finite Element Modeling	17
2.5 Formulation of four node quadrilateral element matrices	17
2.5.1 Shape Functions	18
2.5.2 Element Stiffness Matrix	20
2.5.3 Stiffness Integration	21
2.5.4 Element Force Vectors	21
2.5.5 Stress Calculation	22
2.6 Evaluation of Global Stiffness Matrix and Load Vector	22
2.7 Treatment of Boundary conditions	23

2.8 Element stress calculation	24
Chapter 3	25
Finite Element Mesh and Its Quality	25
3.1 Why we chose to use quadrilateral element	25
3.2 Mesh and its generation	26
3.2.1 Types of Mesh	26
3.2.2 Use of mesh	28
3.2.3 Various Mesh Generation Techniques	29
3.2.3.1 Triangular Meshing	29
3.2.3.2 Quadrilateral Meshing	31
3.3 Mesh quality	32
3.3.1 Element quality	33
3.3.1.1 Distortion Factor	33
3.3.1.2 Aspect ratio	35
3.3.1.3 Computer program “MESH QUALITY_2012”	35
3.3.2 Enough number of element in the mesh	35
Chapter 4	36
Problem Description, Results and Discussions	36
4.1 Problem Description	36
4.2 Basic Physical Model	36
4.2.1 Application of Boundary Condition	38
4.2.2 Application of Loading	39
4.2.3 Finite Element Analysis of the Model of Fig. 4.1 and Discussion on results	39
4.2.3.1 Model 1	39
4.2.3.2 Model 2	45
4.2.3.3 Model 3	49
4.2.3.4 Model 4	53
4.2.4 Finite Element Analysis of a Plate with a center hole and additional holes in a plane perpendicular to the loading direction	57
4.2.5 Verification of the Infiniteness of the Model	63
4.2.6 Von Mises Stress	65

Chapter 5	69
Conclusion and Recommendation	69
5.1 Conclusion	69
5.2 Recommendation for Further Study	70
References	72
Appendix	75

Abstract

In this dissertation, the effect of mesh quality on stress concentration factor in structural discontinuities has been investigated. The effect of mesh quality on stress concentration around the circular holes in an infinite plate subjected to uniform tensile force at the edges of the plate, which very much conforms to the structural problems faced in configuring the structures with discontinuity is highly significant. Because structural discontinuity problems are difficult to solve analytically, a leading general purpose finite element software NASTRAN-PATRAN has been presented to perform the analyses computationally. The main purpose of this thesis is to determine how structural discontinuities alter stress distributions and how the mesh quality influences these stresses. Different models have been used in this study with variable number and quality of elements from model to model. Four-node quadrilateral membrane element (2 degrees of freedom per node) has been used in meshing the computational domain. The mesh quality has been defined as a combination of two criteria such as element quality and enough number of elements in the mesh. The quality of the surface mesh should be good to get acceptable finite element results. Element quality is defined by two factors namely: Distortion factor and Aspect ratio. Based on these two factors an object oriented C++ program named “MESH QUALITY_2012” has been developed. The results have been shown in tabular form and graphically. The computed results show good agreement with the published theoretical results. Finally a correct meshing approach is prescribed to model structures with single or multiple holes which is essential for a finite element analyst.

Declaration

It is hereby declared that the work which is being presented in this dissertation entitled **“Study of the effect of mesh quality on stress concentration factor of plates with holes using finite element analysis”** submitted in partial fulfillment of the requirement for the award of the degree of Master of Philosophy in Mathematics in the Department of Mathematics, Bangladesh University of Engineering & Technology, Dhaka is an authentic record of my own work.

This thesis or any part of it has not been submitted elsewhere (University or Institution) for the award of any degree or diploma.

Date: November, 2012

Sharaban Thohura

Acknowledgement

All praises and gratitude belong to Allah (Most Gracious and Most Merciful) for making things and situations congenial and favorable for me to complete this thesis.

First of all I would like to express my indebtedness to my respected supervisor Dr. Md. Manirul Alam Sarker, Professor, Department of Mathematics and co-supervisor Dr. Md. Shahidul Islam, Associate Professor, Department of Naval Architecture and Marine Engineering, Bangladesh University of Engineering and Technology, Dhaka, Bangladesh. Especially, I acknowledge my gratitude to Dr. Islam for his tireless guidance and support throughout the research. His time input and advise were of immense help in completing this thesis in due time and I will be ever grateful to him.

Besides I would like to be grateful to all of my teachers in the Department of Mathematics, BUET, for their kind help and cooperation.

I would like to express cordial thanks to my colleagues and friends in Jagannath University, Dhaka and Stamford University, Bangladesh for their support and cooperation at different times.

Finally, I express my hearty gratitude to all of my family members for their spontaneous and unbounded love, continuous encouragement and kind cooperation during the entire period of my study.

Sharaban Thohura

November, 2012

Nomenclature

A	Plate length
B	Element strain-displacement matrix
d	Hole diameter
E	Modulus of Elasticity
f	distributed body force per unit volume
F	Global load vector
H	Plate width
I	second moment of area of cross-section of beam about the neutral axis
K	Global Stiffness Matrix
K_{tg}	Stress concentration factor
k^e	Element stiffness matrix
M	Applied bending moment
N	number of degrees of freedom
N_i	Shape function
P_i	Force acting at point i
Q	Global displacement vector
q	Element displacement vector
T	Traction force per unit area
t	Thickness of the plates
t_e	Thickness of element e
u	Displacement of an interior point
U	Strain energy
y	distance of point considered from neutral axis

Greek symbols

σ	<i>Stress</i>
S_{\max}	Maximum stress

S_x	Normal stress in x-direction
S_y	Normal stress in y-direction
S_z	Normal stress in z-direction
S_Y	Yield stress of the material
S_{VM}	Von Mises stress
t_{xy}	Shear stress along xy plane
t_{yz}	Shear stress along yz plane
t_{zx}	Shear stress along zx plane
ε	Normal strain
Π	Potential energy
x	Natural coordinate
ν	Poisson's ratio
h	Natural coordinate

List of Tables

Table No.	Caption	Page No.
4.1	Summary of models and their out put	56
4.2	Stress concentration factor in terms of Von Mises stress	68

List of Figures

Figure	Caption	Page No.
1.1	Vertical shear and longitudinal bending in still water	2
1.2	Wave bending moments	3
1.3	Plate with hole subjected to a tensile force	4
1.4	Fatigue Cracks under combined torsional and axial loading for circular notch/indention	5
1.5	Some ship structures with holes	6
2.1	A three dimensional body	16
2.2	Four-node quadrilateral element	18
2.3	The quadrilateral element in ξ, η space (master element)	19
3.1	Examples of mesh generation	26
3.2	Structured Mesh	27
3.3	Unstructured Mesh	28
3.4	A triangular element is converted into three quadrilateral elements	29
3.5	Derivation of Distortion factor for a quadrilateral element	34
3.6	Elements with unacceptable aspect ratio	35
4.1	Plane stress of a finite width element with a circular hole.	37
4.2	Boundary conditions of models	38
4.3	model -1	40
4.4	Result of model 1	44
4.5	Mesh seed for model 2	45
4.6	Model 2	46
4.7	Result of model 2	48
4.8	Result of model 3	49
4.9	Mesh for model 3	50
4.10	Result of model 3	52
4.11	Mesh of model 4	54
4.12	Result of model 4	55

4.13	A plate with a center hole and additional holes in a plane perpendicular to the loading direction	57
4.14	Mesh seed for model with additional hole	58
4.15	Mesh of model with additional hole	59
4.16	Mesh of model (with element numbers) with additional hole	61
4.17	Result of model with additional hole	62
4.18	Plate (finite length) with hole	63
4.19	Plate (finite length) with hole (Von Mises stress)	64
4.20	Plate (finite length) with hole Maximum stress (X Component)	64
4.21	Von mises stress for model 1	66
4.22	Von mises stress for model 2	66
4.23	Von mises stress for model 3	67
4.24	Von mises stress for model 4	67
4.25	Von mises stress for model with additional hole	68

CHAPTER 1

INTRODUCTION AND LITERATURE REVIEW

1.1 Introduction

The application of finite element method (FEM) to the analysis of discontinuous structural systems has received a significant interest in recent years. Examples of problems in which discontinuities play prominent role in the physical behavior of a system are numerous. In engineering practice, there is a variety of structures with discontinuities. From a mathematical point of view, analytical solutions are possible only for a limited class of such problems. The complexities of the structures, material properties and of boundary conditions, have progressively led to the predominance of numerical models based on finite elements and finite differences. For cases in which discrete representation of discontinuities is required, the finite element approach provides the best modeling to date.

A ship floating in still water has an unevenly distributed weight owing to both cargo distribution and structural distribution. The buoyancy distribution is also non-uniform since the underwater sectional area is not constant along the length. Total weight and total buoyancy are of course balanced, but at each section there will be a resultant force or load, either an excess of buoyancy or excess of load. Since the vessel remains intact there are vertical upward and downward forces tending to distort the vessel (Fig 1.1) which are referred to as vertical shearing forces, since they tend to shear the vertical material in the hull. The ship shown in Figure 1.1 will be loaded in a similar manner to the beam shown below it, and will tend to bend in a similar manner owing to the variation in vertical loading. It can be seen that the upper fibres of the beam would be in tension; similarly the material forming the deck of the ship with this loading. Conversely the lower fibres of the beam, and likewise the material forming the bottom of the ship, will be in compression. A vessel bending in this manner is said to be ‘hogging’ and if it takes up the reverse form with excess weight amidships is said to be ‘sagging’. When sagging the deck will be in compression and the bottom shell in tension.

Lying in still water the vessel is subjected to bending moments, either hogging or sagging depending on the relative weight and buoyancy forces.

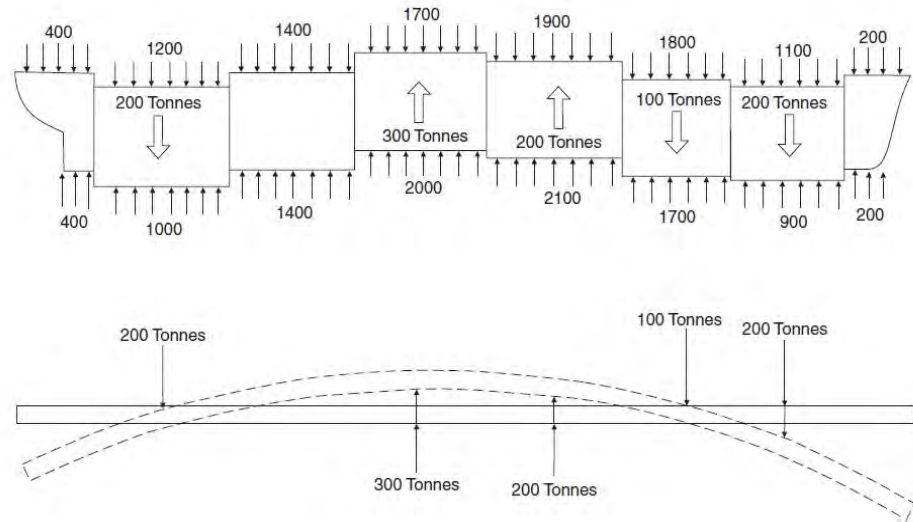


Fig 1.1 Vertical shear and longitudinal bending in still water

When a ship is in a seaway the waves with their troughs and crests produce a greater variation in the buoyant forces and therefore can increase the bending moment, vertical shear force, and stresses. Classically the extreme effects can be illustrated with the vessel balanced on a wave of length equal to that of the ship. If the crest of the wave is amidships the buoyancy forces will tend to ‘hog’ the vessel; if the trough is amidships the buoyancy forces will tend to ‘sag’ the ship (Fig 1.2). In a seaway the overall effect is an increase of bending moment from that in still water when the greater buoyancy variation is taken into account. From classic bending theory the bending stress (σ) at any point in a beam is given by:

$$S = \frac{My}{I}$$

where M =applied bending moment.

y =distance of point considered from neutral axis and

I =second moment of area of cross-section of beam about the neutral axis.

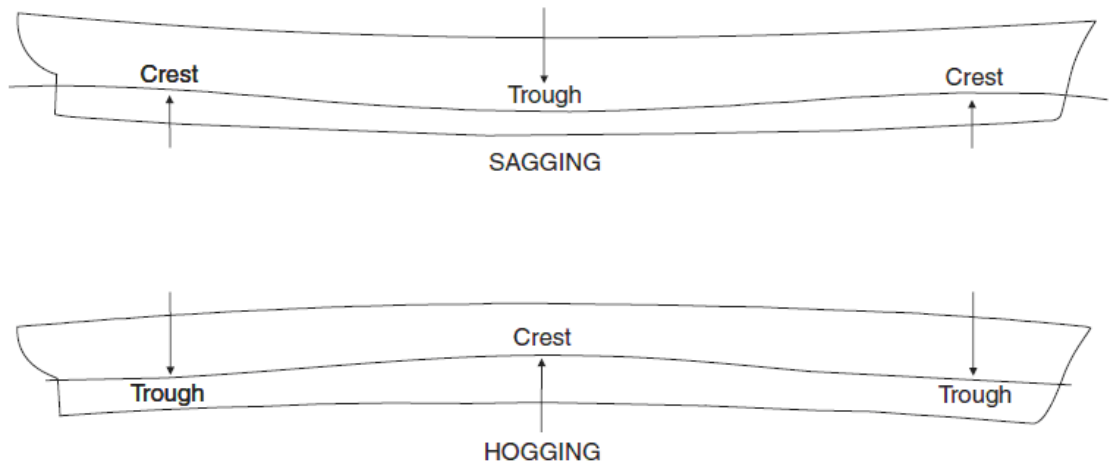


Fig. 1.2 Wave bending moments

When the beam bends it is seen that the extreme fibres are, say in the case of hogging, in tension at the top and in compression at the bottom. Somewhere between the two there is a position where the fibres are neither in tension nor compression. This position is called the *neutral axis*, and at the farthest fibres from the neutral axis, the greatest stress occurs for plane bending. So the deck plate, bottom shell and the members attached to these are in tension or compression and are considered as stressed structural members.

Openings in ship structures are made for access, cargo handling, passage of pipes, ducts and cables, drainage and air escape, weld relief, etc.

In the Maritime and aerospace industry, it is often desirable to design structure to be as light as possible for both performance and cost reasons; a weight reduction can enable ships or airplanes to increase their performance by running on less fuel. By removing small amounts of material from various places in the airframe or in the ship, the total weight of the entire structure can be reduced which decreases the operating cost. In addition to weight concerns, holes may be needed for such reasons as openings for windows and doors or when component are immersed together.

Any opening in a stressed structural member, no matter how small or how well designed and fabricated, always causes a stress concentration. Ship openings that are improperly designed poorly located or involve bad workmanship in cutting and welding may lead to serious structural failures.

If a discontinuity like hole exists in a structural or machine element that interrupts the stress path, then the stress at the discontinuity may be significantly higher than the nominal stress on the section. A stress concentration thus occurs at the discontinuity.

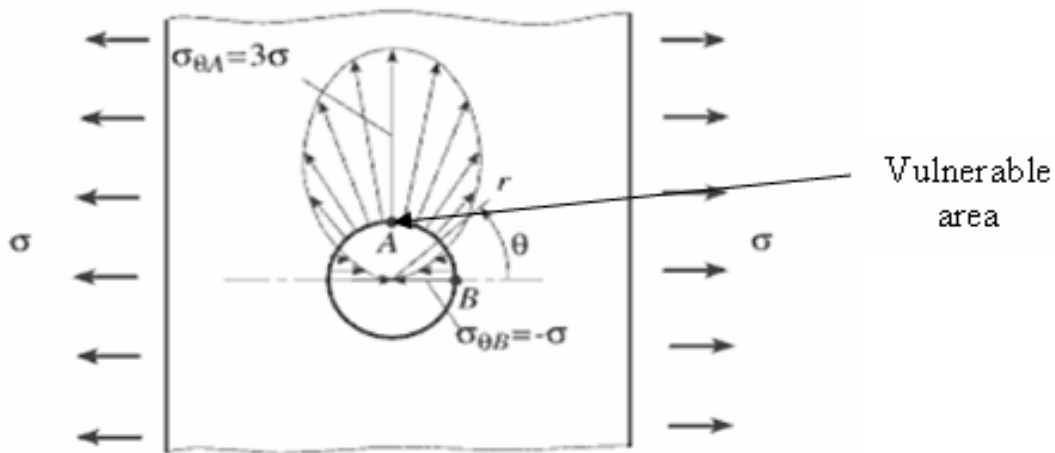


Fig 1.3 Plate with hole subjected to a tensile force

Fig 1.3 shows a plate with a hole subjected to a tensile force. The material which is subjected to a quite low stress may locally be stressed very highly because of discontinuity created by the hole. When these holes are in hull, bending stress levels that are already high, critical stress situations can develop.

By contrast, a less desirable, and unintentional, type of discontinuity that structural engineers have to deal with is cracks, which are usually due to material imperfections that are impossible to avoid. If the stress were so great or below the yield point for the material fatigue failure or local failure might occur which could result in general failure of the structure as shown in the following figure. Although ideally engineers would prefer their structures to be free of cracks, their presence does not necessarily assure that a structure will fail. However, when cracks are detected, certain measures should be taken to determine the probability of crack propagation.

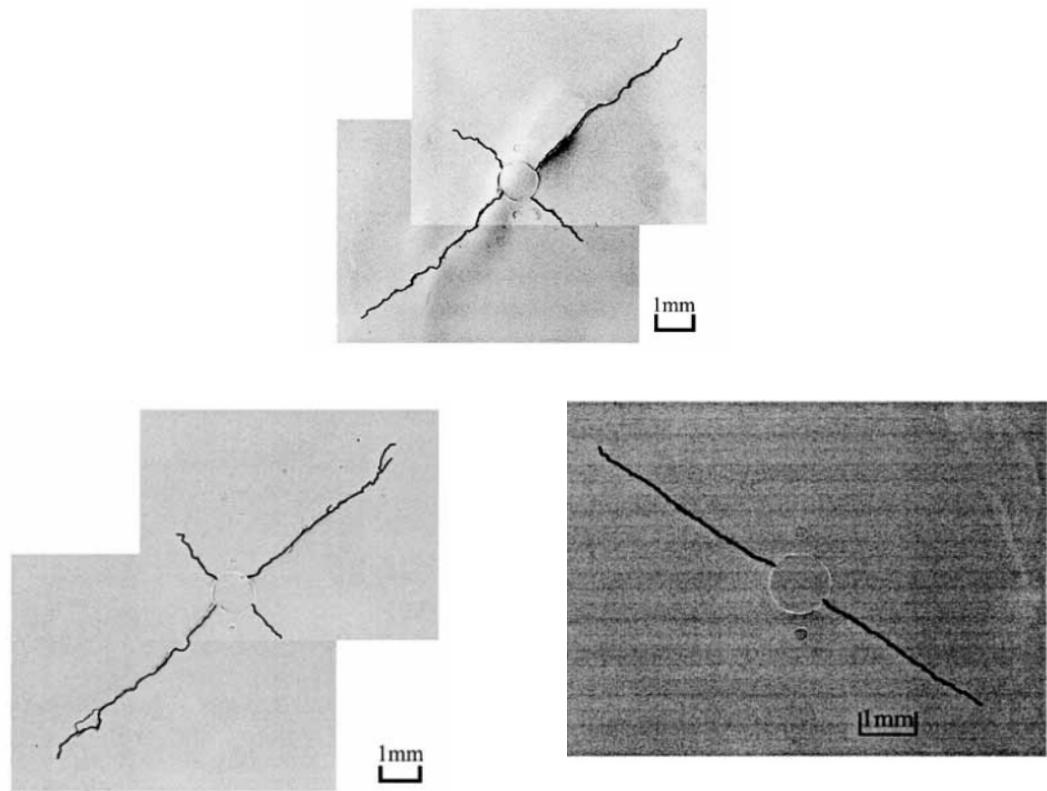


Fig 1.4: Fatigue Cracks under combined torsional and axial loading for circular notch/indentation

The two structural features described above, holes and cracks, are examples of what are known as structural discontinuities. A structural discontinuity can be described as a break or gap in a structural component that alters its behavior when loaded. Configuring the structures with discontinuities is one of the most important topics in the construction of ships, aero-planes, cars etc. Whenever the cross-section of a structural member changes suddenly, a structural discontinuity arises, e.g. deck openings like hatch and machinery openings, access openings on side wall, cutout in the web plate, oil hole in crankshaft etc.



Fig 1.5 Some ship structures with holes

Since structural discontinuities alter the stress distribution of a structure, they also induce stress concentrations such as at the tip of a crack or near the edge of a hole. In the design and testing process, it is these areas of high stress that are of most concern; therefore, an accurate method must be employed to analyze the effects of these discontinuities so that engineers may design around them.

1.2 Review of the previous work:

Considering the importance of structural discontinuity, an extensive research work has been carried out by naval architects, offshore and ocean engineers, hydro dynamists and mathematicians. In the past, stress analyses were performed analytically or experimentally, which could be both difficult and time consuming, especially when dealing with discontinuities. Many times, an accurate solution was not possible due to the complexity of the discontinuity configurations. Stress concentration factors are obtained analytically from the elasticity theory, computationally from the finite element method, and experimentally using methods such as photoelasticity or strain gages. The universal availability of powerful, effective computational capabilities, usually based on the finite element method, has alerted the use of and the need for stress concentration factors. Often a computational stress analysis of a mechanical device, including highly stressed regions, is performed, and the explicit use of stress concentration factors is avoided. Alternatively, a computational analysis can provide stress concentration factor, which is available for traditional design studies. The use of experimental techniques such as photoelasticity to determine stress concentration factors has been virtually replaced by the more flexible and more efficient computational techniques. However, with the advent of the finite element method (FEM), these analyses can now be performed with a great degree of accuracy.

A great many researchers have outlined the importance of stress concentration factor in isotropic and composite materials. Folias and Wang (1990) presented most of the previous works on stress concentration in this subject. They presented a series solution for stress filled around a circular holes in a plates with arbitrary thickness. A wide range of holes diameters to plate thickness are presented. Ko (1985) used anisotropic plate theory to evaluate the stress concentration factor for a single layer or laminated composite plates with central circular cutout. Most of these works are based on the theory developed by Lekhnitskii (1961) and Savin (1961) for perforated anisotropic plates. In all of these works, circular and elliptical cutouts are considered. Daoust and Hoa (1991) solved the case of circular and triangular cutouts and investigated the influence of blunt curvature and material properties on the state of stress around a triangular cutout in an infinite composite plate. Wu and Mu (2003) investigated the stress concentration factor

for isotropic plates under uni-axial and bi-axial loads. The stress concentration factor was also determined for isotropic and orthotropic cylindrical shells with circular cutout. Chai (1996) presented finite element and some experimental results on the free vibration of symmetric composite plates with central hole. Huang and Sakiyama (1999) have proposed an approximate method for analyzing the free vibration of rectangular plates with different cutouts. Delale *et al.* (1984) have considered the axisymmetric bending problem of a perforated plate consisting of two bonded isotropic dissimilar materials. Fraser (1975) considered the problem of finding the stress distribution in a highly stretched plate containing an eccentrically plate-reinforced circular hole subjected to a large biaxial stress system at infinity. Reissner (1975) evaluated the stress concentration factor of an infinite plate containing a circular hole subjected to pure bending using his theory; he has shown that his results are in close agreement with those of Alblas (1957). Lekhnitskii (1968) studied homogenous anisotropic plate with a circular hole subjected to a pure bending moment acting along the edges of the plates.

Iwaki (1980) worked on stress concentrations in a plate with two unequal circular holes. Ukadgaonker and Rao (2000) proposed a general solution for stresses around holes in symmetric laminates by introducing a general form of mapping function and an arbitrary biaxial loading condition into the boundary conditions. Ting *et al.* (1999) presented a theory for stress analysis by using rhombic array of alternating method for multiple circular holes. Chaudhuri (1987) worked on stress concentration around a part through hole weakening a laminated plate by finite element method. Mahiou and Bekaou (1997) studied local stress concentration for the prediction of tensile failure in unidirectional composites. Toubal *et al.* (2005) studied experimentally stress concentration in a circular hole in composite plate. Younis (2006) investigated through reflected photo elasticity method that the assembly stresses contributes in reducing stresses around the holes in a plate. Peterson (1966) has developed good theory and charts on the basis of mathematical analysis and presented excellent methodology in graphical form for evaluation of stress concentration factors in isotropic plates with different types of abrupt change, but no techniques are presented for evaluation of the stress concentration factor in orthotropic and laminated plate. N.K. Jain and N.D. Mittal (2008) have analyzed the effect of D/A ratio (where D is hole diameter and A is plate width) upon stress concentration factor

(SCF) and deflection in isotropic, orthotropic and laminated composite plates with central circular hole under different transverse static loading condition using finite element formulation. Recently, Ulku babuscu yesil (2010) has studied the effect of the initial stretching of the rectangular plate with a cylindrical hole on the stress and displacement distributions around the hole. In order to find the solution of his problem the 3D finite element was employed. Mittelstedt et al. (2004) have presented a closed-form higher-order plate theory approach to find stress concentration in layered plates. Allam et al. (2003) have determined the stress concentration factor for a fiber-reinforced viscoelastic plate using the method of effective moduli. The plate is weakened by an oval or crack opening and deformed by forces applied to its middle plane. A comparison has been made between results when the small oval opening tends to a crack.

1.3 Objectives of this thesis:

A plate with central circular hole have found widespread applications in various fields of engineering such as aerospace, marine, automobile and mechanical. Stress concentration arises from any abrupt change in geometry of plate under loading. As a result, stress distribution is not uniform throughout the cross-section. Failures such as fatigue cracking and plastic deformation frequently occur at points of stress concentration. Hence for the design of a plate with central circular hole, stress concentration plays an important role and accurate knowledge of stresses and stress concentration factor at the edges of hole under in plane or transverse loading are required. Analytical solutions are available in literature for the prediction of stress concentration factor in different types of abrupt changes in shape.

From the discussions made in section 1.2, it is clear that much work has been done on the theoretical development of different stress concentration problems but the effect of mesh quality on the finite element analysis result is never made. To get accurate result in less modeling time is very important in the industries now a day. Trial-error method to get better result is no more possible. For this reason the knowledge of the effect of different shapes of elements of the mesh is very important for a finite element analyst. Without this knowledge erroneous result can be produced which can lead to design of a faulty structure.

In the present work, the stress concentration around the hole in an infinite plate will be investigated using finite element method and the effect of mesh quality on stress concentration factor will be studied as well. The main objective of this study is to analyze the stress concentration around the hole in an infinite plate and to assess the effect of mesh quality on stress concentration factor in finite element method.

The major objectives of this study are:

- § To make a finite element model of a rectangular plate with a circular hole and analyze it to find out stress concentration factor and compare it with the value found from the formula given by Pilkey & Pilkey (2008).
- § To assign appropriate boundary conditions for the model.
- § To produce various models with variable number of grids/nodes.
- § To investigate the effect of mesh quality on the stress concentration factor achieved through finite element analysis.
- § To make finite element models of a rectangular plate for multiple holes

1.4 Outline of Methodology:

This study concerns mainly with the fundamentals of FEM, where a particular structural problem is analyzed to study the effect of mesh quality. The problem involving stress distribution in an infinitely long plate with a hole subjected to uniform tensile force at the edges of the plate is investigated with the help of a FEM based software package- NASTRAN-PATRAN. The approach of solving the problem will be as follows:

- § Different models will be used in this study with variable number and quality of elements from model to model.
- § Four-node quadrilateral membrane element (2 degrees of freedom per node) will be used in meshing the computational domain.
- § The theoretical investigation is being carried out using the formula given by Pilkey & Pilkey (2008).
- § The quality of mesh will be examined using aspect ratio and distortion factor applying program codes written in c++.

- § The results will be shown in tabular form and graphically by utilizing a world renowned and leading general purpose finite element software package NASTRAN-PATRAN.
- § Results will be analyzed specially emphasizing the physical aspects.

1.5 Thesis Framework:

For complete understanding of the work, the thesis is divided into a number of chapters describing its different topics.

Chapter one first discusses on the importance of the study of structural discontinuities and presents the review of previous works on this topic. From these discussions it is clear that much work has been done on the theoretical development of different stress concentration problems but the effect of mesh quality on the finite element analysis result is never made. To get accurate result in less modeling time is very important in the industries. Trial-error method to get better result is no more possible. For this reason the knowledge of the effect of different shapes of elements of the mesh is very important for a finite element analyst. Without this knowledge erroneous result can be produced which can lead to design of a faulty structure. The objectives and outline of the methodology are given in details in later part of the chapter.

In the second chapter some fundamental concepts of finite element method are given. The formulation of quadrilateral element is discussed in details as this element is used in the analytical work of this thesis.

In chapter 3 the importance of choosing quadrilateral element over triangular element in 2-D finite element analysis is presented. Different mesh generation procedures are discussed to understand why the shape of the elements may not become perfect. The mesh quality and element quality are then discussed. The standard of element quality (distortion factor and aspect ratio) is first fixed and then the developed computer program “**MESH QUALITY_2012**” is discussed.

Following this, the formulation and modeling of the problem, as mentioned above, are being carried out in Chapter 4. In this chapter we have also mentioned our results in both tabular and graphical form.

And at last conclusion of our findings with future recommendations on further study in the field of Finite Element analysis are discussed in Chapter 5.

CHAPTER 2

BASICS OF FINITE ELEMENT METHOD

In this thesis we used finite element method (FEM) for analyzing structural discontinuities problems. To facilitate the study some basic concepts of FEM are discussed below.

2.1 What is The Finite Element Method (FEM)?

The Finite Element Method originated as a method of stress analysis. Today finite elements are also used to analyze problems of heat transfer, fluid flow, lubrication, electric and magnetic fields and many others. This method is used to model a structure as an assemblage of small elements. Each element is of simple geometry and therefore is much easier to analyze than the actual structure. Then analyzing those elements individually and taking into account the interactions between them, the solution of that specified problem can be obtained.

The finite element procedure produces many simultaneous algebraic equations, where the calculations are performed on personal computers, mainframes and all sizes in between. Results are rarely exact. However, errors are decreased by processing more equations and results accurate enough for engineering purposes are obtainable at reasonable cost.

Now-a-days most of the analysis using FEM is done on software packages, which comprises of mainly three components – pre-processor, solver and post-processor. These components usually perform the functions followed by a typical finite element analysis, where the steps that are pursued to do so are given below:

- At first the structure or continuum has to be discretized into finite elements. Mesh generation program, called Pre-processors, help the user in doing so. Then the boundary conditions and known nodal values (for plane stress problem it is zero, for heat transfer problem it is the nodal temperature) are specified on the mesh to assign it the correct nodal degrees of freedom.

- In the next step simultaneous linear algebraic equations, evolved from various elements, are solved by the program called 'Solver' to determine the specific nodal values, which depends upon the nature of the problem (for plane stress problem it is nodal stress value, for heat transfer problem it is the nodal heat fluxes, etc.).
- Last step concerns the generation of output (as determined by the solver) in a graphical form with the help of an output interpretation program, called Post-processor.

The power of the finite element method resides principally in its versatility. The method can be applied to various physical problems. The body analyzed can have arbitrary shape, loads and boundary conditions. The mesh can mix elements of different types, shapes and physical properties. This great versatility may be contained within a single computer program. User-prepared input data controls the selection of problem type, geometry, boundary conditions, element selection and so on.

Another attractive feature of finite element method is the close physical resemblance between the actual structures and its finite element model. The model is not simply an abstraction. This seems especially true in structural mechanics and may account for the finite element method having its origins here.

2.2 How/Why should we study the method?

Whether computer based or not, analytical methods rely on assumptions and on theory that is not universally applicable. That is why its limitations are really a matter to be concerned with. It is far easier for a user to make silly mistakes like making an error in computer program, input of wrong data or generation of poor mesh, which would lead to the formation of incorrect output with elegant graphic display. The results obtained from the programs cannot be trusted if user has no knowledge of their internal workings and little understanding of the physical theories on which those are based. Moreover, the choice of element for various analyses is crucial. An element that is good in one problem area (such as magnetic fields) may be poor in another (such as stress analysis). Even in a specific problem area an element may behave well or badly, depending on particular geometry, loading and boundary conditions. If an analysis is to be done by numerical

methods, finite elements are not the only choice, because there are other methods like finite difference method, boundary element method, finite volume method etc., which would be more effective in some areas of analysis than the finite element method. For example, finite difference methods are effective for shell of revolutions and boundary elements are effective for some problems with boundaries at infinity. But in linear computational solid mechanics problems, finite element methods currently dominate the scene as regards space discretization. Boundary element methods post a strong second choice in specific application areas, where for nonlinear problems the dominance of finite element method is overwhelming. In other cases experiment may be the most appropriate method to obtain data needed for analysis, as well as to compare it with the results obtained from analysis using the discretization methods, where the analytical process is being pushed beyond previous experience & established practice.

2.3 Fundamentals of Finite Element Method

As mentioned earlier in Section 2.1 that the FEM analysis of the structural problem involves three major steps - the tasks involved in each step require a good understanding of the sequential aggregation of the modeling of the structure. Preprocessing involves the preparation of data, such as nodal connectivity, boundary conditions, and loading and material information. The processing stage involves stiffness generation, stiffness modification and the solution of the equations, resulting in the evaluation of the nodal variables. Other derived quantities, such as gradients or stresses, may be evaluated at this stage. The postprocessing stage deals with the presentation of results. Typically, the deformed configuration, mode shapes, temperature, and stress distribution are computed and displayed at this stage. A complete Finite Element Analysis is a logical interaction of three stages. Since this study mainly focuses on the two-dimensional problem concerning the analysis of a plate with a hole, the approach towards most of the conceptual review would be to cover only the two-dimensional aspects of finite element analysis.

Today the concept of the finite element method is a very broad one. Even when restricting ourselves to the analysis of structural mechanics problems only, the approach towards the formulation of those can differ in nature. Here the potential energy approach

is being applied in the derivation of necessary entities, needed in solving those analytical problems.

The formulation of element stiffness matrix and global load vector requires the potential energy or variational approach, where the potential energy is defined as,

$$\tilde{O} = \frac{1}{2} \int_v \delta \boldsymbol{\sigma}^T \boldsymbol{\varepsilon} dV - \int_v \delta \mathbf{u}^T \mathbf{f} dV - \int_s \delta \mathbf{u}^T \mathbf{T} dS - \sum_i \delta \mathbf{u}_i^T \mathbf{P}_i \quad (2.1)$$

where, the first term denotes the strain energy equation for a linear elastic body, which is expressed as,

$$U = \frac{1}{2} \int_v \boldsymbol{\sigma}^T \boldsymbol{\varepsilon} dV \quad (2.2)$$

and the rest of the terms together constitute the work potential of the body, where

$$\mathbf{WP} = - \int_v \delta \mathbf{u}^T \mathbf{f} dV - \int_s \delta \mathbf{u}^T \mathbf{T} dS - \sum_i \delta \mathbf{u}_i^T \mathbf{P}_i \quad (2.3)$$

In equation (2.1), \mathbf{f} & \mathbf{T} denotes the body force components comprising the distributed forces per unit volume and surface traction forces per unit area respectively as shown in Fig-2.1. Here the Fig-2.1 represents a three-dimensional body having a volume and surface area V and S respectively. Traction force per unit area \mathbf{T} and distributed body force per unit volume \mathbf{f} , are also shown in the figure, where some region of the boundary, S_u , are constrained. The deformation of a point $\mathbf{x} (= [x, y, z]^T)$ is given by the three components of its displacements, $\mathbf{u} = [u, v, w]^T$. In the last term of equation (2.1), \mathbf{P}_i represents a force acting at point i .

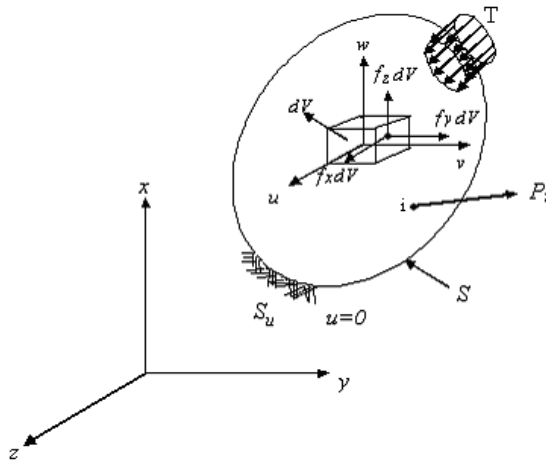


Fig-2.1: A three dimensional body

2.4 Finite Element Modeling

The Finite Element Method is the dominant discretization technique in structural mechanics. The basic concept in FEM is the subdivision of a region into disjoint (non-overlapping) components of simple geometry called finite element or element for short. For 2-D modeling the most commonly employed elements are linear or quadratic triangles and quadrilaterals. In two-dimensional problem, each node is permitted to displace in the two directions. Thus, each node has two degrees of freedom. So, the displacement components of node j are taken as Q_{2j-1} in the x direction and Q_{2j} in the y direction. And the global displacement vector can be represented as

$$\mathbf{Q} = [Q_1, Q_2, \dots, Q_N] \quad (2.4)$$

and global load vector,

$$\mathbf{F} = [F_1, F_2, \dots, F_N] \quad (2.5)$$

where N is the number of degrees of freedom (d.o.f), which is defined as the flexibility of the nodes to displace in permitted numbers of direction. Thus in two dimensional problem, as the nodes are permitted to displace in both $\pm x$ and $\pm y$ direction, hence each node has two degrees of freedom.

Computationally, the information on the discretization is to be represented in the form of *nodal coordinates* and *connectivity*. The nodal coordinates are stored in a two-dimensional array represented by the total number of nodes and the two coordinates per node. The element connectivity information is an array of the size and number of elements and the nodes per element, which are the global node numbers of the particular elements that can be derived from the discretized region.

2.5 Formulation of four node quadrilateral element matrices:

The two dimensional Finite Element formulation provides with a family of Isoparametric elements, where the Four-node Quadrilateral Element represents one of the most basic form among those. Since in this study the discretization of the models are made using the quadrilateral elements, the shape functions, element stiffness matrix and element body forces for only this particular element is being figured out here.

Here a general quadrilateral element has been considered as shown in Fig-2.2, having local nodes numbered as 1,2,3 and 4 in a counterclockwise fashion and (x_i, y_i) are the coordinates of node i . The vector $\mathbf{q} = [q_1, q_2, \dots, q_8]^T$ denotes the element displacement vector. The displacement of an interior point P located at (x, y) is represented as $\mathbf{u} = [u(x, y), v(x, y)]^T$.

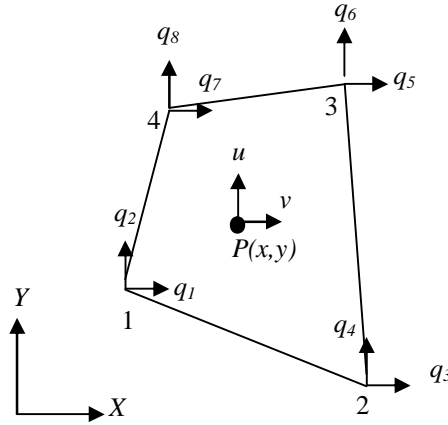


Fig 2.2: Four-node quadrilateral element

2.5.1 Shape Functions

To develop the shape functions let us consider a master element (Fig-2.3) having a square shape and being defined in ζ -, η - coordinates (or natural coordinates). The Lagrange shape functions, where $i = 1, 2, 3$ and 4 , are defined such that N_i is equal to unity at node i and is zero at other nodes. In particular:

$$N_1 = \begin{cases} 1, & \text{at node 1} \\ 0, & \text{at node 2, 3 and 4} \end{cases} \quad (2.6)$$

Now, the requirement that $N_1 = 0$ at nodes 2, 3 and 4 is equivalent to requiring that $N_1 = 0$ along edges $\zeta = +1$ and $\eta = +1$ (Fig-2.3.).

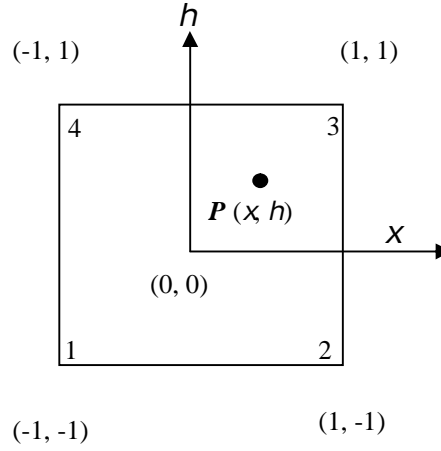


Fig 2.3: The quadrilateral element in ξ, η space (master element)

All the four shape functions can be written as

$$\begin{aligned}
 N_1 &= \frac{1}{4}(1-x)(1-h) & N_2 &= \frac{1}{4}(1+x)(1-h) \\
 N_3 &= \frac{1}{4}(1+x)(1+h) & N_4 &= \frac{1}{4}(1-x)(1+h)
 \end{aligned}
 \tag{2.7}$$

Now, to express the displacement field within the element in terms of the nodal values, let $\mathbf{u} = [u, v]^T$ represent the displacement components of a point located at (ξ, η) , and \mathbf{q} , dimension (8×1) , represents the element displacement vector which can be written in matrix form as,

$$u = Nq \tag{2.8}$$

where,

$$N = \begin{bmatrix} N_1 & 0 & N_2 & 0 & N_3 & 0 & N_4 & 0 \\ 0 & N_1 & 0 & N_2 & 0 & N_3 & 0 & N_4 \end{bmatrix} \begin{matrix} \hat{u} \\ \hat{v} \end{matrix}
 \tag{2.9}$$

In the isoparametric formulation, the same shape functions can also be used to express the coordinates of a point within the element in terms of nodal coordinates.

Thus,

$$\begin{aligned}
 x &= N_1x_1 + N_2x_2 + N_3x_3 + N_4x_4 \\
 y &= N_1y_1 + N_2y_2 + N_3y_3 + N_4y_4
 \end{aligned}
 \tag{2.10}$$

Let a function $f = f(x, y)$, in view of Equation (2.10) be considered to be an implicit function of x and h as

$$f = f[x(x, h), y(x, h)]. \quad (2.11)$$

From calculus we find that

$$dx dy = \det \mathbf{J} dx dh \quad (2.12)$$

where, \mathbf{J} is the Jacobian matrix.

$$\mathbf{J} = \begin{bmatrix} \frac{\partial x}{\partial x} & \frac{\partial y}{\partial x} \\ \frac{\partial x}{\partial h} & \frac{\partial y}{\partial h} \end{bmatrix} \begin{bmatrix} \dot{u} \\ \dot{v} \end{bmatrix} \quad (2.13)$$

2.5.2 Element Stiffness Matrix

The stiffness matrix for the quadrilateral element can be derived from the strain energy in the body, given by,

$$U = \int_V \frac{1}{2} \sigma^T \varepsilon dV \quad (2.14)$$

or,

$$U = \int_e t_e \int_e \frac{1}{2} \sigma^T \varepsilon dA \quad (2.15)$$

where t_e is the thickness of element e . Using the strain-displacement relation the strain in the element is expressed in terms of its nodal displacement. The stress is now given by

$$\sigma = \mathbf{D} \mathbf{B} \mathbf{q} \quad (2.16)$$

where, \mathbf{D} is a (3×3) material matrix. energy in equation (2.15) becomes,

$$U = \int_e t_e \int_e \frac{1}{2} \sigma^T \varepsilon dx dy \quad (2.17)$$

As, $\sigma^T = \mathbf{D} \mathbf{q}^T \mathbf{B}^T$ and $\varepsilon = \mathbf{B} \mathbf{q}$, using equation (2.15) we get,

$$U = \int_e \frac{1}{2} \mathbf{q}^T \begin{bmatrix} \frac{\partial}{\partial x} & \frac{\partial}{\partial y} \\ \frac{\partial}{\partial x} & \frac{\partial}{\partial y} \\ \frac{\partial}{\partial x} & \frac{\partial}{\partial y} \end{bmatrix} \mathbf{B}^T \mathbf{D} \mathbf{B} \det \mathbf{J} dx dh \begin{bmatrix} \dot{u} \\ \dot{v} \end{bmatrix} \quad (2.18)$$

$$U = \int_e \frac{1}{2} \mathbf{q}^T \mathbf{k}^e \mathbf{q} \quad (2.19)$$

where,

$$k^e = t_e \int_{-1}^1 \int_{-1}^1 \mathbf{B}^T \mathbf{D} \mathbf{B} \det \mathbf{J} d\xi d\eta \quad (2.20)$$

is the element stiffness matrix of dimension (8×8).

Here the quantities \mathbf{B} and $\det \mathbf{J}$ in the integral in equation (2.20) are involved functions of ξ and η .

2.5.3 Stiffness Integration

From equation (2.20) we find the element stiffness for a quadrilateral element

$$\mathbf{k}^e = t_e \int_{-1}^1 \int_{-1}^1 \mathbf{B}^T \mathbf{D} \mathbf{B} \det \mathbf{J} dx dh \quad (2.21)$$

where \mathbf{B} and $\det \mathbf{J}$ are functions of ξ and η . This integral actually consists of the integral of each element in an (8×8) matrix. The Gaussian quadrature approach for evaluating this integral is adopted here. This method has proved most useful in finite element work.

2.5.4 Element Force Vectors

Body Force

A body force that is distributed force per unit volume, contributes to the global load vector \mathbf{F} . This contribution can be determined by considering the body force term in the potential – energy expressions

$$\int_V \mathbf{u}^T \mathbf{f} dV \quad (2.22)$$

Using $\mathbf{u} = \mathbf{N}\mathbf{q}$, and treating body force $\mathbf{f} = [f_x, f_y]^T$ as constant within each element, we get

$$\int_V \mathbf{u}^T \mathbf{f} dV = \sum_e \mathbf{q}^T \mathbf{f}^e \quad (2.23)$$

where the (8×1) element body force vector is given by,

$$\mathbf{f}^e = t_e \int_{-1}^1 \int_{-1}^1 \mathbf{N}^T \det \mathbf{J} dx dh \begin{bmatrix} \tilde{u} f_x \\ \tilde{u} f_y \end{bmatrix} \quad (2.24)$$

Since \mathbf{N}^T and $\det \mathbf{J}$ is the function of ξ and η , the body force vector has to be evaluated numerically.

Traction Force

A traction force is distributed load acting on the surface of the body. Such a force acts on edges connecting boundary nodes. A traction force acting on the edge of an element contributes to the global load vector \mathbf{F} . Let us assume a traction force

$\mathbf{T} = [T_x, T_y]^T$ is applied on edge 2-3 of the quadrilateral element in Fig-2.3. From the potential energy equation we get the traction term,

$$\int_L \mathbf{Q}^T \mathbf{T} t_e dl = \int_{\Omega_{2-3}} (uT_x + vT_y) t_e dl \quad (2.25)$$

Along that edge we have $\xi = 1$. If we use the shape functions as in equation (2.7), this becomes $N_1 = N_4 = 0$, $N_2 = (1-\eta)/2$ and $N_3 = (1 + \eta)/2$, where the shape functions have become linear functions. Consequently, from the potential, the element traction load vector is readily given by,

$$\mathbf{T}^e = \frac{t_e l_{2-3}}{2} [0 \ 0 \ T_{x2} \ T_{y2} \ T_{x3} \ T_{y3} \ 0 \ 0]^T \quad (2.26)$$

where, l_{2-3} = length of edge 2-3. T_{x2} , T_{x3} are the traction force components at node 2 and T_{y2} , T_{y3} are the traction force components at node 3.

Finally, point loads are considered in the usual manner by having a structural node at that point and simply adding to the global load vector \mathbf{F} .

2.5.5 Stress Calculation

From equation (2.16) we get that, the stresses $\sigma = \mathbf{DBq}$ acting in the quadrilateral element are not constant within the element; they are functions of ξ and η and consequently vary within the element. In practice, the stresses are evaluated at the Gauss points, which are also the points used for numerical evaluation of \mathbf{k}_e , where they are found to be accurate.

2.6 Evaluation of Global Stiffness Matrix and Load Vector

This section explains the way to assemble the Global Stiffness Matrix and Load Vector.

The total potential energy as in equation (2.1) can be written in the form,

$$\tilde{\mathbf{O}} = \frac{1}{2} \mathbf{Q}^T \mathbf{K} \mathbf{Q} - \mathbf{Q}^T \mathbf{F} \quad (2.27)$$

by taking element connectivity into account, where \mathbf{K} and \mathbf{F} are the Global Stiffness Matrix and Load Vector respectively. This step involves assembling \mathbf{K} and \mathbf{F} from element stiffness and force matrices. The global load vector \mathbf{F} is assembled from element force vectors and point loads as-

$$\mathbf{F} = \mathring{\mathbf{a}}_e (\mathbf{f}^e + \mathbf{T}^e) + \mathbf{P}_i \quad (2.28)$$

where, \mathbf{f}^e & \mathbf{T}^e are the element body force vector and element traction force vector respectively and \mathbf{P}_i represents the point vector.

2.7 Treatment of Boundary conditions:

In dealing with the proper boundary condition and deriving the equilibrium equations the minimum potential energy theorem can be used. This theorem states that: *Of all possible displacements that satisfy the boundary conditions of a structural system, those corresponding to equilibrium configurations make the total potential energy assume a minimum value.* Consequently, the equations of equilibrium can be obtained by minimizing with respect to Q , the potential energy P subject to the boundary conditions. Boundary conditions are usually of the type,

$$Q_{p1} = a_1, Q_{p2} = a_2, \dots, Q_{pr} = a_r \quad (2.29)$$

where, P_1, P_2, \dots, P_r are denoted to be the degrees of freedom and r is judged to be the number of supports in the structure. The requirement that the potential energy P takes on a minimum value is obtained from the equation.

$$\frac{dP}{dQ_i} = 0 \quad i = 2, 3, \dots, N \quad (2.30)$$

Applying these boundary conditions and also using the equation 2.30 the finite **element equations** can be expressed in the matrix form as,

$$\mathbf{K} \mathbf{Q} = \mathbf{F} \quad (2.31)$$

where, \mathbf{K} is a reduced $(N-1 \times N-1)$ matrix obtained by eliminating the row and column corresponding to the specified degrees of freedom. This process of determining equilibrium equations is referred to as **elimination approach**.

In the elimination approach, the stiffness matrix \mathbf{K} is obtained by deleting rows and columns corresponding to fixed d.o.f.

2.8 Element stress calculation

Equation (2.31) can be solved for the displacement vector \mathbf{Q} using Gaussian elimination. As the reduced \mathbf{K} matrix is a nonsingular one, the boundary condition can be considered to be specified properly. Once \mathbf{Q} has been determined, the element stress can be evaluated using the equation derived from Hooke's law,

$$\sigma = E\mathbf{B}\mathbf{q} \tag{2.32}$$

where \mathbf{B} is the element strain-displacement matrix and \mathbf{q} is the element displacement vector for each element, which is extracted from \mathbf{Q} using element connectivity information.

CHAPTER 3

FINITE ELEMENT MESH AND ITS QUALITY

It has been already mentioned that for finite element analysis, the problem domain need to be discretized or subdivided into disjoint (non-overlapping) components of simple geometry called finite element or element for short. Moreover for two dimensional finite element analyses there exist principally two types of elements, triangular and quadrilateral elements. In section 2.5 we mentioned that we will use 4 node quadrilateral elements for our analysis in this thesis. In this chapter we will focus on the advantages of quadrilateral elements over triangular elements and the domain discretization techniques which are also called finite element meshing.

3.1 Why we chose to use quadrilateral element?

Consideration of the convergence characteristics of two dimensional solutions of elastic continuum problems, using both quadrilateral and triangular elements, has been covered in previous studies and some finite element textbooks (Zienkiewicz and Taylor 1989, Brauer 1993). Such studies conclude that the significant factors that affect convergence characteristics of finite element solutions include the element's basic shape, element distortion, polynomial order of the element, completeness of polynomial functions, integration techniques, and material incompressibility. It is generally accepted that simplex triangular elements are inferior when compared to bilinear quadrilaterals. For example, statements such as "... for reasons of better accuracy and efficiency, quadrilateral elements are preferred for two- dimensional meshes and hexahedral elements for three-dimensional meshes. This preference is clear in structural analysis and seems to also hold for other engineering disciplines." (Brauer, 1993) However, it is also generally accepted that triangular elements, with higher order displacement assumptions, provide acceptable accuracy and convergence characteristics. However, mesh locking due to material incompressibility as reported by Hughes(1987), is a serious shortcoming of triangular elements.

3.2 Mesh and its generation

A key step of the finite element method for numerical computation is mesh generation. Mesh generation is the practice of generating a [polygonal](#) or [polyhedral mesh](#) that approximates a geometric domain. In this process, one is given a domain (such as a polygon or polyhedron; more realistic versions of the problem allow curved domain boundaries) and must partition it into simple "elements" meeting in well-defined ways. There should be few elements, but some portions of the domain may need small elements so that the computation is more accurate there. All elements should be "well shaped" (which means different things in different situations, but generally involves bounds on the angles or aspect ratio of the elements).

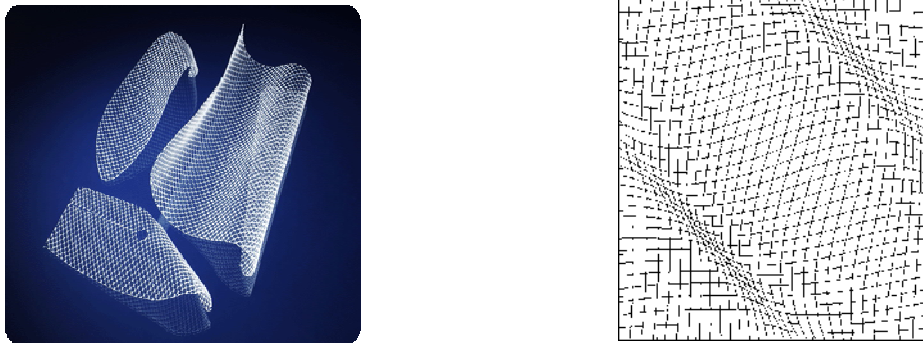


Fig 3.1: Examples of mesh generation

3.2.1 Types of Mesh

From the point of view of how elements meet, mesh can be divided into two major types:

1. Structured Mesh: A structured mesh can be recognized by all interior nodes of the mesh having an equal number of adjacent elements. For this purposes, the mesh generated by a structured grid generator is typically all quad or hexahedral. Algorithms employed generally involve complex iterative smoothing techniques that attempt to align elements with boundaries or physical domains. Where non-trivial boundaries are required, “block structured” techniques can be employed which allow the user to break the domain up into topological blocks. Structured grid generators are most commonly used within the CFD field, where strict alignment of elements can be required by the analysis code or necessary to capture physical phenomenon.

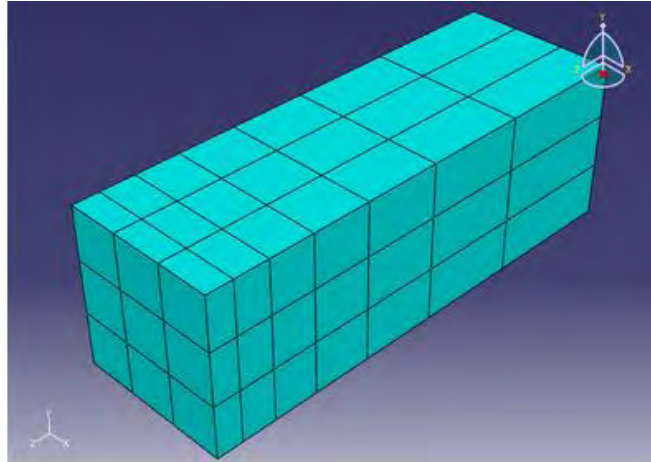


Fig 3.2: Structured Mesh

2. Unstructured Mesh: An unstructured (or irregular) grid is a [tessellation](#) of a part of the [Euclidean plane](#) or [Euclidean space](#) by simple shapes, such as [triangles](#) or [tetrahedra](#), in an irregular pattern. Grids of this type may be used in [finite element analysis](#) when the input to be analyzed has an irregular shape.

In Unstructured mesh generation relaxes the node valence requirement, allowing any number of elements to meet at a single node. Triangle and Tetrahedral meshes are most commonly thought of when referring to unstructured meshing, although quadrilateral and hexahedral meshes can also be unstructured. While there is certainly some overlap between structured and unstructured mesh generation technologies, the main feature which distinguish the two fields are the unique iterative smoothing algorithms employed by structured grid generators.

Unlike [structured grids](#), unstructured grids require a list of the [connectivity](#) which specifies the way a given set of vertices make up individual elements.

[Ruppert's algorithm](#) is often used to convert an irregularly shaped polygon into an unstructured grid of triangles.

In addition to triangles and tetrahedra, other commonly used elements in finite element simulation include quadrilateral (4-noded) and hexahedral (8-noded) elements in 2D and 3D, respectively. One of the most commonly used algorithms to generate unstructured quadrilateral grid is "Paving". However, there is no such commonly used algorithm for generating unstructured hexahedral grid on a general 3D solid model. "Plastering" is a 3D

version of Paving, but it has difficulty in forming hexahedral elements at the interior of a solid.

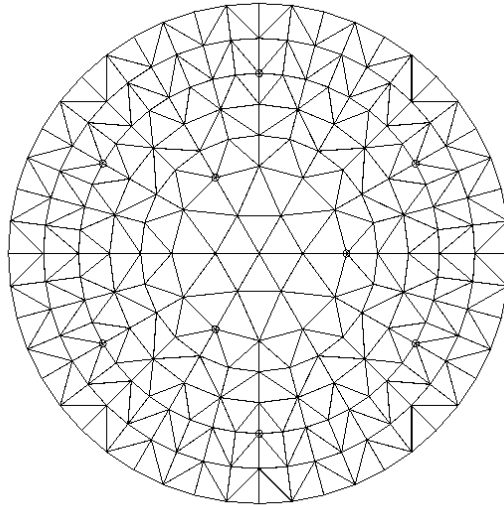


Fig 3.3: Unstructured Mesh

3.2.2 Use of mesh:

Typical uses of mesh are for rendering to a computer screen or for physical simulation such as [finite element analysis](#) or [computational fluid dynamics](#). The field is highly interdisciplinary, with contributions found in [mathematics](#), [computer science](#), and [engineering](#). There has now been considerable theoretical work in the geometry community on mesh generation problems, complementing and building on practical work in the numerical community. There is also beginning to be a convergence of these communities, in which theoretical work is fed back in to practical mesh generation applications. Theoretically, the preferred type of mesh is the triangulation, but in mesh generation practice quadrilaterals or higher dimensional cubical element shapes are preferred (both because fewer are typically needed and because they have better numerical properties). Remaining problem areas in the theory of meshing include triangulations in dimensions higher than two, meshes with cubical elements, mesh smoothing, mesh decimation and multi-grid methods, and data structures for efficient implementation of meshing algorithms. There has also been some theoretical work on

using geometry to partition meshes by finding small separators of their underlying graphs.

3.2.3 Various Mesh Generation Techniques

In this section we will discuss triangular (three noded) and quadrilateral (four noded) mesh generation techniques (two dimensional linear elements). In section 3.1 above we stated that we are going to use quadrilateral mesh for our analysis. But it is important to mention that a triangle can be subdivided into quadrilaterals (that is, a triangular mesh can be converted into quadrilateral mesh), thus their (triangular elements) generation is also relevant and important.

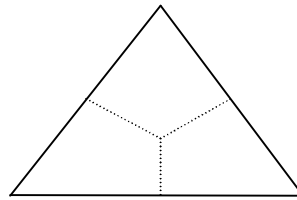


Fig 3.4: A triangular element is converted into three quadrilateral elements

3.2.3.1 Triangular Meshing

Triangles are by far the most common forms of two dimensional unstructured mesh generation. There are a number of triangulation techniques. We will discuss the following techniques:

- a. Delaunay
- b. Octree
- c. Advancing Front
- d. Islam et al.(2010) proposed technique

a. Delaunay

The Delaunay Method is one of the most popular techniques of triangular mesh generation. In [mathematics](#) and [computational geometry](#), a Delaunay triangulation for a set \mathbf{P} of points in the plane is a [triangulation](#) $DT(\mathbf{P})$ such that no point in \mathbf{P} is inside the [circumcircle](#) of any [triangle](#) in $DT(\mathbf{P})$, i.e., Delaunay criterion is the requirement that the circumcircles of all triangles have empty interiors. It was given by Boris Delaunay in 1934.

The criterion in itself is not an algorithm for generating a mesh. It merely provides the criterion for which to connect a set of existing points in space. As such it is necessary to provide a method for generating node locations within the geometry. A typical approach is to first mesh the boundary of the geometry to provide an initial set of nodes. The domain bounded by boundary nodes is then triangulated according to the Delaunay criterion which involves Voroni diagram. In two dimensions the Voroni diagram of a group of vertices divides two dimensional space into regions bound by straight line segments. Each region or Voroni cell belongs to one vertex. Although the Delaunay criterion has been known for many years, it was not until the work of Lawson (1977) and Watson (1981) that the criterion was utilized for developing algorithms to triangulate a set of vertices. The criterion was later used in developing meshing algorithms by Baker (1989) at Princeton, Weatherill and Hassan (1994) at Swansea, George et. al. (1991) at IRINA among others.

Delaunay triangulations maximize the minimum angle of all the angles of the triangles in the triangulation; they tend to avoid skinny triangles.

b. Octree

The Octree technique was primarily developed in the 1980s by Mark Shephard at Rensselaer. With this method, cubes containing the geometric model are recursively subdivided until the desired resolution is reached. First the equivalent two-dimensional quadtree decomposition of a model is taken. Irregular cells are then created where cubes intersect the surface, often requiring a significant number of surface intersection calculations. Tetrahedra are generated from both the irregular cells on the boundary and the internal regular cells. The Octree technique does not match a pre-defined surface mesh, as an advancing front or Delaunay mesh might, rather surface facets are formed wherever the internal octree structure intersects the boundary. The resulting mesh also will change as the orientation of the cubes in the octree structure is changed and can also require. To ensure element sizes do not change too dramatically, a maximum difference in octree subdivision level between adjacent cubes can be limited to one. Smoothing and cleanup operations can also be employed to improve element shapes.

c. Advancing Front

Another very popular family of triangle and tetrahedral mesh generation algorithms is the advancing front, or moving front method. It was first presented by Lo in 1985. He presented a new mesh generation algorithm that initially defines the boundary of the domain by a set of line segments, the initial advancing front. All nodes are generated within the domain bounded by the initial advancing front and valid triangular elements are then formed from the line segments and interior nodes. Each element is generated by joining the end nodes of a line segment to a third node with the condition that it does not intersect the advancing front. The front is then updated and the element creation process goes on as long as the front is not empty. Peraire et al [9] presented a modified version of advancing front method in 1987. Most of the subsequent advancing front method research has been based upon Peraire's algorithm.

d. Islam et al.(2010) proposed technique

A triangular mesh generation algorithm was presented by Islam et al.(2010). On that procedure a fully automatic object oriented program in C++ language was developed for any arbitrary 2D geometry. The program generates unstructured triangular surface mesh which can be used for finite element analysis. The program gives mesh output in a script file format for viewing in AutoCAD. Importance is given to the quality of the triangles generated so that better results can be achieved by the finite element analysis. A very practical approach has been taken in this regard. A number of example meshes were presented to show the effectiveness of the algorithm and program.

3.2.3.2 Quadrilateral Meshing

Automatic unstructured mesh generation algorithms have lent themselves more readily to triangle and tetrahedral meshing. As a result, most of the literature and software are triangle and tetrahedral. In spite of this, there is a significant group of literature that focuses on unstructured quad and hexahedral methods. Unstructured quad34 and hex35 meshing software have also become widely available in recent years. Unlike triangle and tetrahedral methods, extension from a 2D quadrilateral algorithm to a 3D hexahedral method is not generally straightforward.

There are two main types of Quad/Hexahedral Meshing:

- a. Mapped Meshing
- b. Unstructured Quad Meshing

a. Mapped Meshing

When the geometry of the domain is applicable, quad or hex mapped meshing³⁶ will generally produce the most desirable result. Although mapped meshing is considered a structured method, it is quite common for unstructured codes to provide a mapped meshing option. For mapped meshing to be applicable, opposite edges of the area to be meshed must have equal numbers of divisions. In 3D, each opposing face of a topological cube must have the same surface mesh. This can often be impossible for an arbitrary geometric configuration or can involve considerable user interaction to decompose geometry into mapped meshable regions and assign boundary intervals. In order to reduce human interaction, research has been done in recent years through the CUBIT³⁷ project at Sandia National Labs to automatically recognize features³⁸ and decompose geometry³⁹ into separate mapped meshable areas and volumes. Work has also been done to automate interval assignments⁴⁰. Another category of mapped meshing, also developed as part of the CUBIT³⁷ project is referred to as submapping⁴¹. This method, rather than decomposing the geometry directly, determines an appropriate *virtual* decomposition based on corner angles and edge directions. The separate map-meshable regions are then meshed separately. This method is suitable for blocky shapes and volumes that have well defined corners and cube-like regions.

b. Unstructured Quad Meshing

Unstructured quadrilateral meshing algorithms can, in general, be grouped into two main categories: direct and indirect approaches. With an indirect approach, the domain is first meshed with triangles. Various algorithms are then employed to convert the triangles into quadrilaterals. With a direct approach, quadrilaterals are placed on the surface directly, without first going through the process of triangle meshing.

3.3 Mesh quality

The title of this thesis is "Study of the Effect of Mesh Quality on Stress concentration factor of plate with holes using Finite Element Analysis". In this section we will discuss how we define mesh quality in our study and why.

We define mesh quality as a combination of two criteria.

1. Element quality
2. Enough number of element in the mesh

3.3.1 Element quality

The quality of the surface mesh should be good to get acceptable finite element results. To judge if a mesh is of sufficient good quality, it is needed to define a standard. Element quality is defined by two factors:

- a. Distortion factor
- b. Aspect ratio

3.3.1.1 Distortion Factor:

Zhu et al (1991) considered a quadrilateral element satisfactory if all its internal angles θ fall within $90^\circ \pm 45^\circ$ and was considered as unsatisfactory if θ exceeds the limit $90^\circ \pm 60^\circ$. Lo and Lee (1992) found that the first condition appeared to be too strict, so a more flexible range of $90^\circ \pm 52.5^\circ$ was used for quadrilateral interior angles. In the present study Lo and Lee's range is chosen for acceptable quality of a quadrilateral element. Any element exceeding this range is considered unacceptable. The optimum shape for a quadrilateral is a square with interior angles 90° . The following equations were used to measure the distortion factor of quadrilaterals.

The deviation of each interior angle of a quadrilateral, dq_i , is defined as,

$$dq_i = \left| \frac{p}{2} - q_i \right| \quad i = 1, 2, 3, 4.$$

The distortion factor for quadrilateral element, F_q is defined as,

$$dq_i = \left| \frac{p}{2} - q_i \right| \quad i = 1, 2, 3, 4.$$

$$F_q = \sqrt{\sum_{i=1}^4 (dq_i)^2}$$

It can be seen that F_q would attain a minimum value of zero for a perfect square and the acceptable range of $90^\circ \pm 52.5^\circ$ defined by Lo and Lee would correspond to $F_q \leq 105^\circ$.

Derivation of Distortion factor for a quadrilateral element (Fig. 3.5) can be expressed in the following manner:

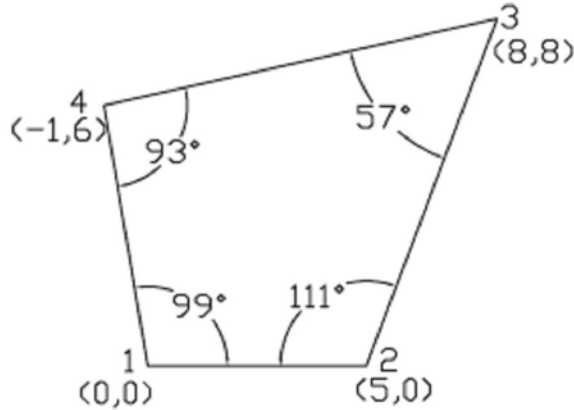


Fig. 3.5 Derivation of Distortion factor for a quadrilateral element

The deviations of each interior angle can be expressed as,

$$dq_1 = |90^\circ - 99^\circ| = 9^\circ$$

$$dq_2 = |90^\circ - 111^\circ| = 21^\circ$$

$$dq_3 = |90^\circ - 57^\circ| = 33^\circ$$

$$dq_4 = |90^\circ - 93^\circ| = 3^\circ$$

Hence, the distortion factor, $F_q = \sqrt{(dq_1^2 + dq_2^2 + dq_3^2 + dq_4^2)}$

$$= \sqrt{(9^2 + 21^2 + 33^2 + 3^2)}$$

$$= 40.25^\circ$$

where, the value of F_q is below the limit of 105° . So, the element as depicted above can be said to possess acceptable quality in terms of distortion factor according to Lo and Lee.

3.3.1.2 Aspect ratio:

Aspect ratio of a quadrilateral element is defined as the ratio of the largest to the smallest length of the sides of the element.

So,

$$\text{Aspect ratio} = L_{\max} / L_{\min}$$

Where, L_{\max} and L_{\min} are the largest and smallest characteristic lengths of an element, respectively. Examples of acceptable and unacceptable elements in terms of aspect ratio are given below:

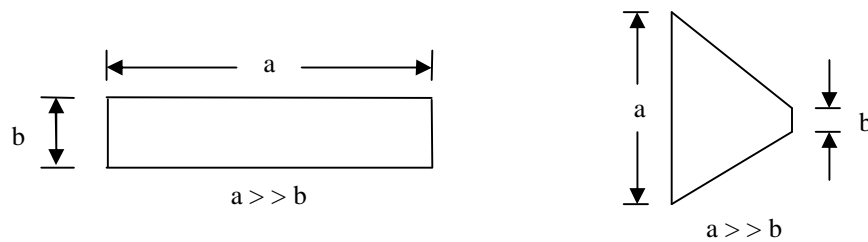


Fig. 3.6 Elements with unacceptable aspect ratio

3.3.1.3 Computer program “MESH QUALITY_2012”

Based on the above two factors an object oriented C++ program named “MESH QUALITY_2012” is developed. The program listing is given in the Appendix. It takes NASTRAN PATRAN *.dat files as input and calculates each element internal angles and computes the distortion factor. Finding out the maximum and minimum edge length of each element it also calculates the aspect ratio. Finally the average distortion factor of the mesh and element of worst distortion factor is found out.

3.3.2 Enough number of element in the mesh

As the results obtained in solving problems by finite element method yield the approximate solution, the convergence towards the exact result necessitates the implementation of enough number of elements in modeling structures. If the number of element is not enough, the exact result will not come and if the number of element is in excess it will cause waste of manpower, time and will require much more computing ability (includes increased use of computer graphics). An example may be to model a part with 10 thousand elements while it can be sufficiently modeled by 5 thousand elements. This can go to much extreme case.

CHAPTER 4

PROBLEM DESCRIPTION, RESULTS AND DISCUSSIONS

4.1 Problem Description

It is known that stress, which is denoted by S , is a function of loading and cross-section area. Therefore, a rectangular plate being loaded uniformly will have a uniform stress distribution as well. However, introducing a structural discontinuity, such as a hole or crack, alters the plate's stress distribution. The reason the stress field is altered is because the presence of the hole requires that the stresses in the plate redistribute themselves in order for any part of the structure to remain in static equilibrium. This phenomenon holds true for cracks as well. Since material is separated in a crack, the structure can no longer carry any loads on these surfaces and stress distribution around the crack will change. This alteration of the stress fields around structural discontinuities induces stress concentrations such as at the tip of a crack or near certain parts of the edge of the hole.

When discontinuities are introduced into a structure, the problem can no longer be solved by simple solid mechanics methods and alternate methods must be employed to reach an accurate solution.

In his chapter, the stress concentration around the hole in an infinite plate will be investigated using finite element method and the results will be compared with theoretical values. The effect of mesh quality on stress concentration factor will be studied as well. Then the acquired knowledge of appropriate meshing for another physical problem will be used for which there is no theoretical study.

4.2 Basic Physical Model

Let an infinitely long plate be of finite width H as in the following Figure, which is being placed under constant tensile stress σ (plane stress), acting in a perpendicular direction to the width at the edges of the plate and having a circular hole of diameter d at the middle of it.

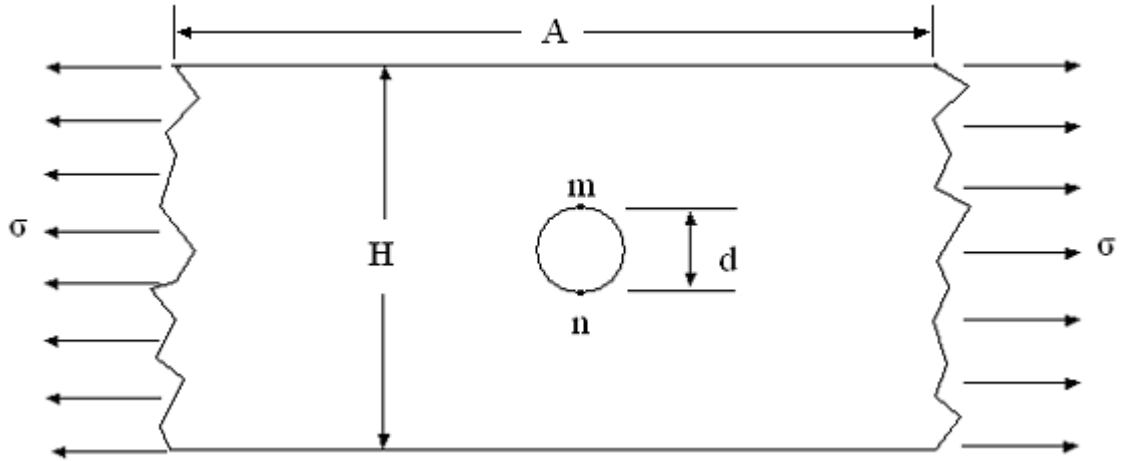


Fig-4.1: Plane stress of a finite width element with a circular hole.

The stress concentration factor k can be defined as the ratio of the maximum stress in the body to some other stress taken as reference stress. The value of this factor depends very much on the abruptness of discontinuity, and it follows that it is desirable to design the structures in the neighborhood of a discontinuity so as to keep this factor as low as possible.

Stress concentration Formula for plate with a hole is defined as (Pilkey & Pilkey, 2008)

$$K_{tg} = \frac{S_{\max}}{S} = 0.284 + \frac{2}{1 - d/H} - 0.600 \frac{d}{H} + 1.32 \frac{d^2}{H^2} \quad (4.1)$$

where K_{tg} is the stress concentration factor based on gross stress, S_{\max} is the maximum stress, at the edge of the hole (at the ends m and n in Fig. 4.1), S is the stress on gross section far from the hole.

Stress concentration factors are obtained analytically from the elasticity theory, computationally from the finite element method and experimentally using methods such as photoelasticity or strain gages. Unfortunately, use of stress concentration factors in analysis and design is not on as firm a foundation as the theoretical basis for determining the factors. In time, advances will take place and revisions in the use of stress concentration factors will need to be made accordingly. On the other hand, it can be said that our limited experience in using these methods has been satisfactory as (Pilkey & Pilkey, 2008).

For modeling purposes, one quarter of plate is being subjected to the analysis due to the symmetrical appearance of the structure about horizontal and vertical axis. Application of uniform stress at the edges was also being applied with the help of symmetrical boundary conditions.

The useful quantities used in this problem are:

- Uniform stress at the edges $\sigma = 400$ psi
- Thickness of the plates $t = 0.4$ inch
- Modulus of Elasticity $E = 30 \times 10^6$ psi
- Poisson's ratio $\nu = 0.3$
- Plate length $A = 20$ inch
- Plate width $H = 20$ inch
- Hole diameter $d = 2$ inch

4.2.1 Application of Boundary Condition

Proper boundary conditions are needed to be applied to make the analysis conforming to the real life experiments. In this respect, the behavior of boundary conditions in this problem is illustrated as follows:

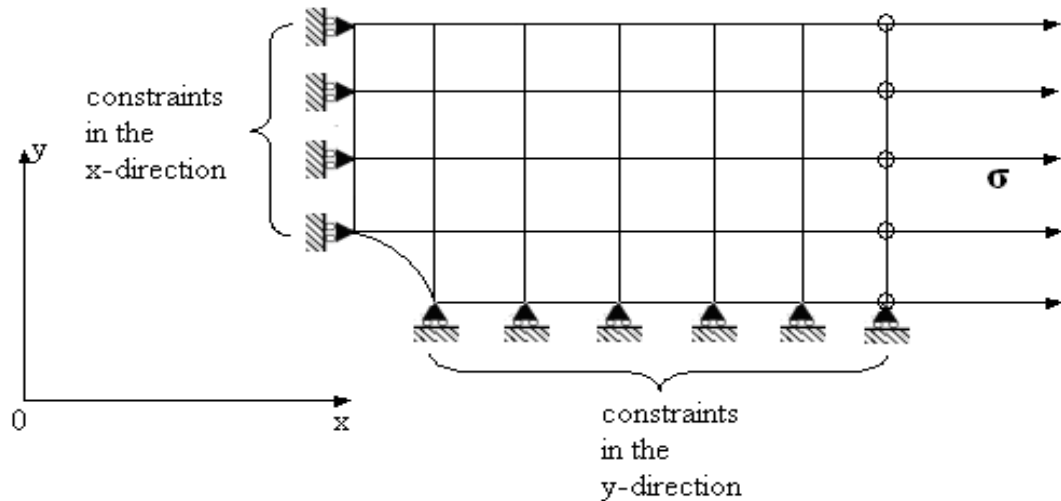


Fig 4.2: Boundary conditions of models

From Fig 4.1 we can see that the geometry of the plate model along with its loading is symmetrical. Now this symmetric property can be fully utilized by modeling only a

quarter model as shown in Fig 4.2 (the mesh shown in Fig 4.2 is just for illustration, actual mesh will be shown in later figures). From this figure it is evident that the sides of the quarter of plates adjacent to the hole are being constrained to move in such directions which would restrict the rigid body displacement of the models.

4.2.2 Application of Loading

Considering the two – dimensional aspect of the problem, the body forces comprising the weights of the plates are neglected, where the Global Load Vector, \mathbf{F} , is deemed to be comprised of only the nodal components of traction forces applied at the edges. The nodal traction force components are obtained using the following formula (we are considering a traction force/pressure is applied on edge 2-3 of a quadrilateral element)

$$T^e = \frac{t_e l_{2-3}}{2} \begin{bmatrix} 0 & 0 & T_{x2} & T_{y2} & T_{x3} & T_{y3} & 0 & 0 \end{bmatrix} \quad (4.2)$$

where, l_{2-3} = length of edge 2 - 3, T_{x2}, T_{y2} are the traction force components at node 2 and T_{x3}, T_{y3} are the traction force components at node 3.

4.2.3 Finite Element Analysis of the Model of Fig. 4.1 and Discussion on results

The finite element analysis software used for this study are NASTRAN-PATRAN. PATRAN is preprocessor and is used for model making and output visualization. NASTRAN is solver. As these are world leading general purpose finite element software, so we use it for most reliable analysis.

4.2.3.1 Model 1

The first finite element model for the problem discussed in the beginning of section 4.2 is shown in Fig 4.3. The model has 27 nodes and 16 quadrilateral elements. The PATRAN *.bdf file (which NASTRAN uses to solve) is then shown. Then the output of our program named MESH QUALITY_2012 is presented.

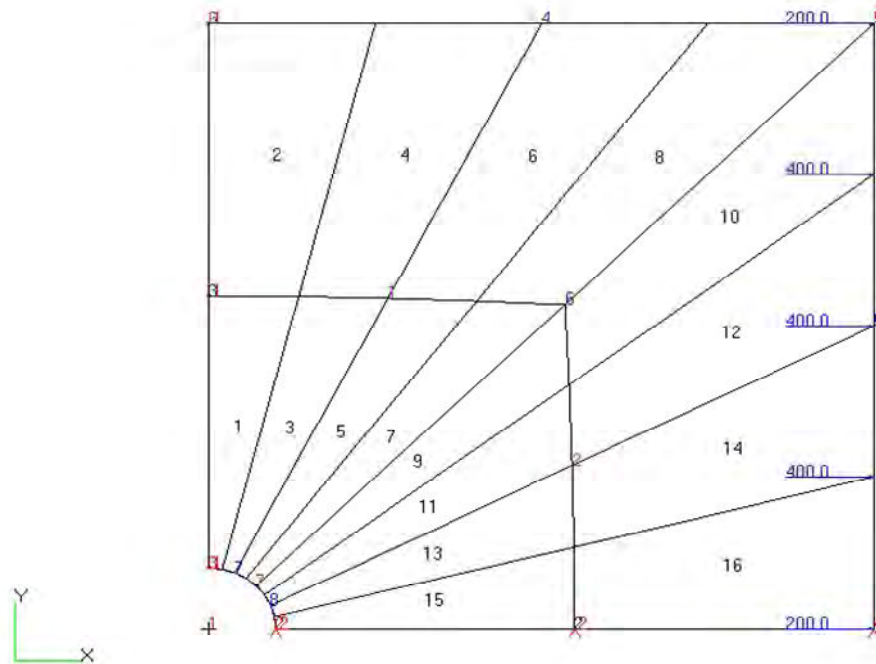


Fig 4.3: model -1

The data file generated for Model- 1(a) by software PATRAN is as follows:

\$ NASTRAN input file created by the MSC MSC.Nastran input file

\$ translator (MSC.Patran 12.0.041).

\$ Direct Text Input for File Management Section

\$ Linear Static Analysis, Database

SOL 101

\$ Direct Text Input for Executive Control

CEND

SEALL = ALL

SUPER = ALL

TITLE = MSC.Nastran job created on 01-Jan-06 at 04:17:00

ECHO = NONE

\$ Direct Text Input for Global Case Control Data

SUBCASE 1

\$ Subcase name : Default

 SUBTITLE=Default

 SPC = 2

 LOAD = 2

```

DISPLACEMENT(SORT1,REAL)=ALL
SPCFORCES(SORT1,REAL)=ALL
STRESS(SORT1,REAL,VONMISES,BILIN)=ALL
BEGIN BULK
PARAM POST 0
PARAM AUTOSPC YES
PARAM PRTMAXIM YES
$ Direct Text Input for Bulk Data
$ Elements and Element Properties for region : ph
PSHELL 1 1 1 .4
$ Pset: "ph" will be imported as: "pshell.1"
CQUAD4 1 1 1 2 5 4
CQUAD4 2 1 2 3 6 5
CQUAD4 3 1 4 5 8 7
CQUAD4 4 1 5 6 9 8
CQUAD4 5 1 7 8 11 10
CQUAD4 6 1 8 9 12 11
CQUAD4 7 1 10 11 14 13
CQUAD4 8 1 11 12 15 14
CQUAD4 9 1 13 14 17 16
CQUAD4 10 1 14 15 18 17
CQUAD4 11 1 16 17 20 19
CQUAD4 12 1 17 18 21 20
CQUAD4 13 1 19 20 23 22
CQUAD4 14 1 20 21 24 23
CQUAD4 15 1 22 23 26 25
CQUAD4 16 1 23 24 27 26
$ Referenced Material Records
$ Material Record : steel
$ Description of Material
MAT1 1 3.+7 .3
$ Nodes of the Entire Model
GRID 1 0. 1. 0.
GRID 2 0. 5.5 0.
GRID 3 0. 10. 0.
GRID 4 .195094 .980785 0.
GRID 5 1.34756 5.49039 0.

```



```

GRID 6      2.5  10.  0.
GRID 7      .38269 .923877 0.
GRID 8      2.69137 5.46194 0.
GRID 9      5.  10.  0.
GRID 10     .55558 .831463 0.
GRID 11     4.02782 5.41573 0.
GRID 12     7.5  10.  0.
GRID 13     .707107 .707107 0.
GRID 14     5.35355 5.35355 0.
GRID 15     10.  10.  0.
GRID 16     .831472 .555567 0.
GRID 17     5.41574 4.02777 0.
GRID 18     10.  7.5  0.
GRID 19     .923882 .382677 0.
GRID 20     5.46194 2.69132 0.
GRID 21     10.  5.  0.
GRID 22     .980788 .195079 0.
GRID 23     5.49039 1.34751 0.
GRID 24     10.  2.5  0.
GRID 25     1.  0.  0.
GRID 26     5.5  0.  0.
GRID 27     10.  0.  0.

$ Loads for Load Case : Default
SPCADD 2 1 3
LOAD 2 1. 1. 1 1. 3
$ Displacement Constraints of Load Set : b2
SPC1 1 1 1 2 3
$ Displacement Constraints of Load Set : b1
SPC1 3 2 25 26 27
$ Nodal Forces of Load Set : p1
FORCE 1 15 0 200. 1. 0. 0.
FORCE 1 27 0 200. 1. 0. 0.
$ Nodal Forces of Load Set : p2
FORCE 3 18 0 400. 1. 0. 0.
FORCE 3 21 0 400. 1. 0. 0.
FORCE 3 24 0 400. 1. 0. 0.

$ Referenced Coordinate Frames

```

ENDDATA

Here CQUAD4 means quadrilateral shaped membrane element. Membrane elements are those which can effectively model in plane loading of plates and formulation of this element is given in Chapter 2.

The output of MESH QUALITY_2012 is as follows:

Quad no	angle1	angle2	angle3	angle4	distortion	factor aspect ratio
1	95.624976	89.591407	76.073021	98.710595	17.367858	23.743039
2	90.408593	90.000000	75.664754	103.926653	19.990445	3.453959
3	92.539813	103.122735	64.248717	100.088734	30.717551	25.972369
4	76.877590	104.335246	63.036367	115.750797	42.045665	3.788034
5	91.161492	114.983810	54.839098	99.015600	44.080720	29.335088
6	65.016676	116.963633	52.859284	125.160407	62.983260	4.300463
7	92.234016	124.455866	47.685345	95.624773	54.903238	33.521971
8	55.544629	127.140716	45.000000	132.314655	79.888268	4.951126
9	95.625150	47.685675	124.455236	92.233939	54.902624	33.519276
10	132.314325	45.000000	127.141173	55.544502	79.888361	4.950938
11	99.016331	54.838970	114.983893	91.160806	44.081001	29.335260
12	125.161293	52.858827	116.964134	65.015746	62.984607	4.300481
13	100.089118	64.249063	103.122327	92.539493	30.717186	25.972084
14	115.751298	63.035866	104.335842	76.876994	42.046683	3.788051
15	98.710630	76.073445	89.591392	95.624533	17.367393	23.744823
16	103.927234	75.664158	90.000000	90.408608	19.991278	3.454096

*****bad quadfaces, distortion factor more than 105(the passing mark).*****

*****average distortion factor and aspect ratio*****

46.930409 17.208737

*****quad with worst distortion factor*****

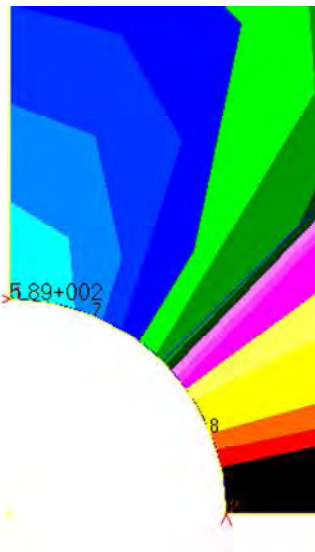
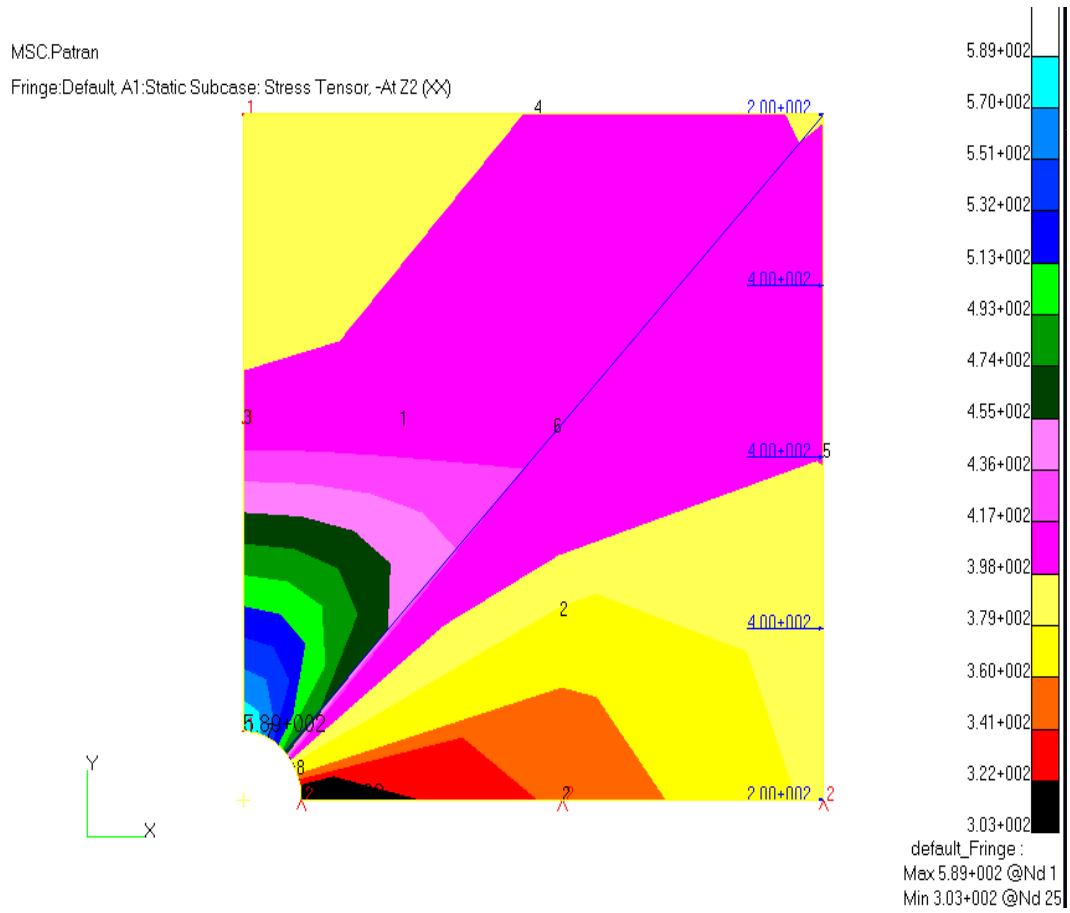
10, 79.888361

*****quad with worst aspect ratio*****

7, 33.521971

From the output of MESH QUALITY_2012 given above, it is seen that the distortion factors of the elements are all within the acceptable range but the aspect ratio of all the elements are too high. Where a value of 5 may be too high, here only 8 elements have aspect ratio below 5.

The result file is shown in Fig 4.4. From the figure it is seen that the maximum stress developed is 589 psi. So the stress concentration factor is $589/400 = 1.4725$.



← Enlarged around the maximum stress

Fig 4.4 Result of model 1

4.2.3.2 Model 2

To create second finite element model for our problem two surfaces were created as in figure below. Each edge is then divided as shown in Fig 4.5. The word ms means mesh seed which represents number of subdivisions. One way bias 1.5 means largest subdivision is 1.5 times larger from the smallest one.

Based on theses seeding the mesh of Fig 4.5 is generated. The model has 99 nodes and 80 quadrilateral elements.

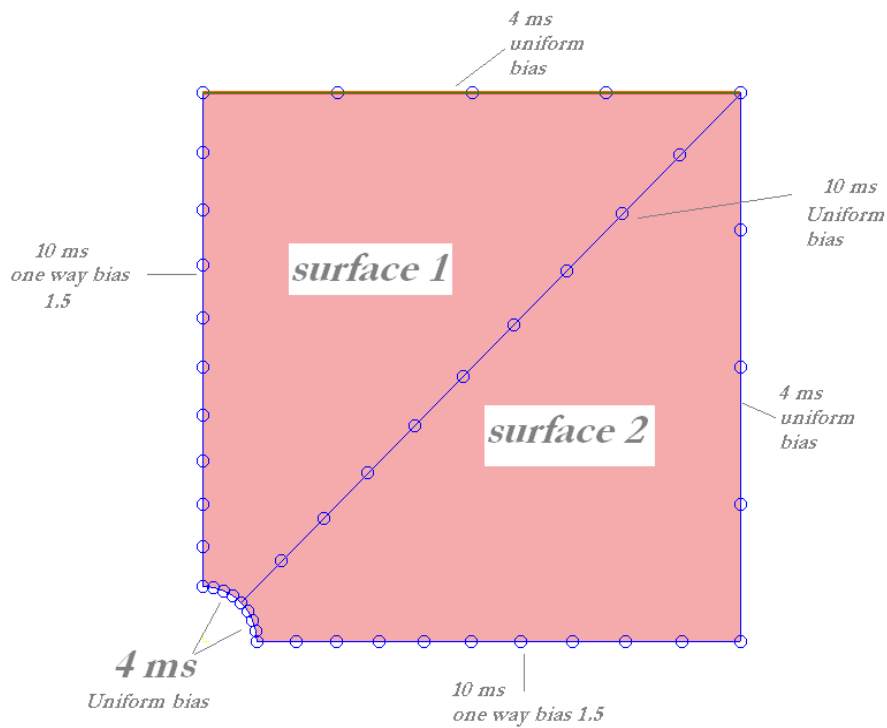


Fig 4.5 Mesh seed for model 2

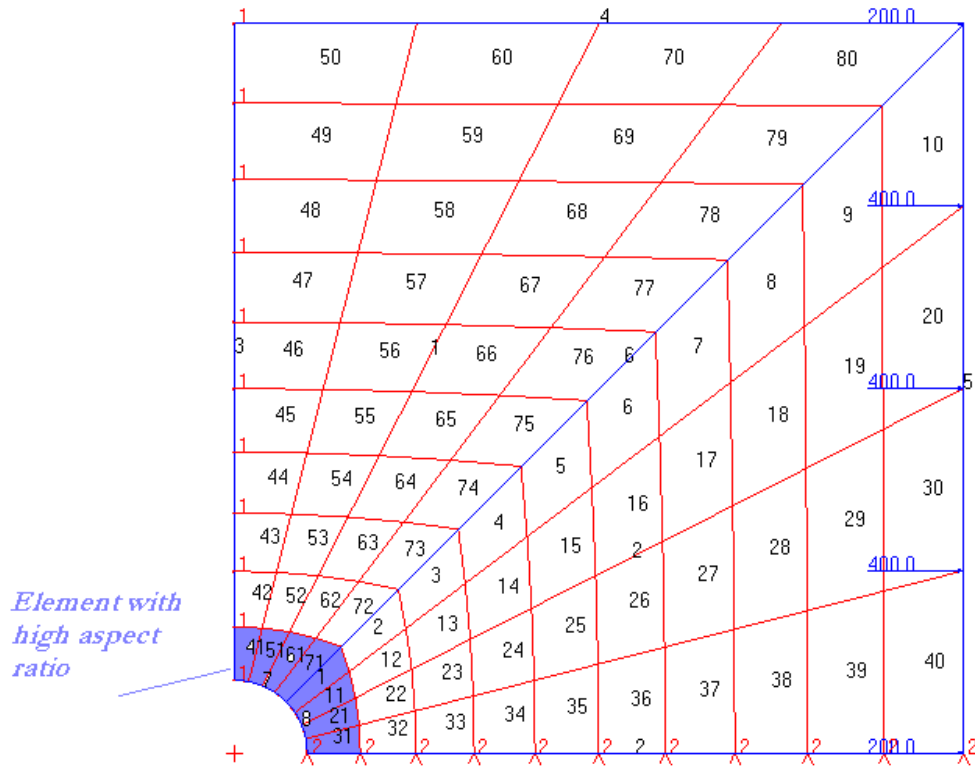


Fig 4.6 Model 2

The output(in short form) of MESH QUALITY_2012 for model 2 is as follows:

quad no,	angle1	angle2	angle3	angle4	distortion	aspect ratio factor
1	95.625150	63.778636	108.341410	92.254804	32.568293	5.428097
2	116.221364	56.132324	115.998948	71.647363	53.360510	3.091528
3	123.867676	52.253277	119.887720	63.991327	64.354964	2.118035
.
.
.
11	98.995466	66.203556	103.626862	91.174116	28.883543	4.759553
21	100.075809	70.906022	96.488863	92.529306	22.684899	4.218154
22	109.101371	67.716005	99.665887	83.516738	31.573737	2.280432
23	112.289619	66.109099	101.262430	80.338852	35.885684	1.574353

28	116.277623	63.452662	103.912036	76.357679	42.129945	1.888878
29	116.541408	63.233878	104.141498	76.083216	42.597305	2.052024
30	116.757154	63.046844	104.345458	75.850545	42.993222	2.206617
31	98.720816	78.045358	87.609293	95.624533	16.009902	3.854348
32	101.949042	76.999741	88.660510	92.390707	17.868857	2.063080
33	102.995520	76.528023	89.136967	91.339490	18.786078	1.427243
40	104.228506	75.654542	90.000000	90.116952	20.205352	2.287073
41	95.624976	87.609462	78.044364	98.721198	16.010983	3.854078
42	92.390538	88.660594	76.999025	101.949843	17.869885	2.062940
43	91.339406	89.137017	76.527368	102.996209	18.787017	1.427158
44	90.862983	89.386467	76.281388	103.469162	19.254604	1.272824
48	90.289517	89.790087	75.877698	104.042699	19.918953	1.953723
49	90.209914	89.883050	75.779963	104.127074	20.045982	2.123878
50	90.116950	90.000000	75.656012	104.227038	20.203274	2.287073
51	92.529210	96.488169	70.906581	100.076039	22.684322	4.218190
52	83.517624	99.665475	67.716814	109.100088	31.572082	2.280434
59	76.083730	104.140983	63.234743	116.540544	42.595886	2.052020
60	75.852015	104.343988	63.047667	116.756329	42.991218	2.206631
61	91.174187	103.627608	66.203390	98.994815	28.883832	4.759524
62	76.365722	109.004086	60.822153	113.808039	44.330783	2.626936
69	63.657168	116.691776	53.132278	126.518778	64.025352	1.874755
70	63.317152	116.952333	52.877447	126.853068	64.611417	2.016304
71	92.254801	108.342272	63.778154	95.624773	32.569101	5.428534
72	71.646299	115.998726	56.133129	116.221846	53.360493	3.091718
73	63.992132	119.887336	52.253661	123.866871	64.353812	2.118186
79	53.661166	126.800539	45.336668	134.201628	81.384198	1.658809
80	53.214115	127.122553	45.000000	134.663332	82.165068	1.786731

*****bad quadfaces, distortion factor more than 105(the passing mark).*****

*****average distortion factor and aspect ratio*****

46.067674 2.060350

*****quad with worst distortion factor*****

10, 82.165659

*****quad with worst aspect ratio*****

71, 5.428534

From the output of MESH QUALITY_2012 for model 2 it is seen that all the elements have acceptable distortion factor but the elements surrounding the hole (the quad no.1, 11, 21, 31, 41, 51, 61, 71) have larger aspect ratio 3.8 to 5.4.

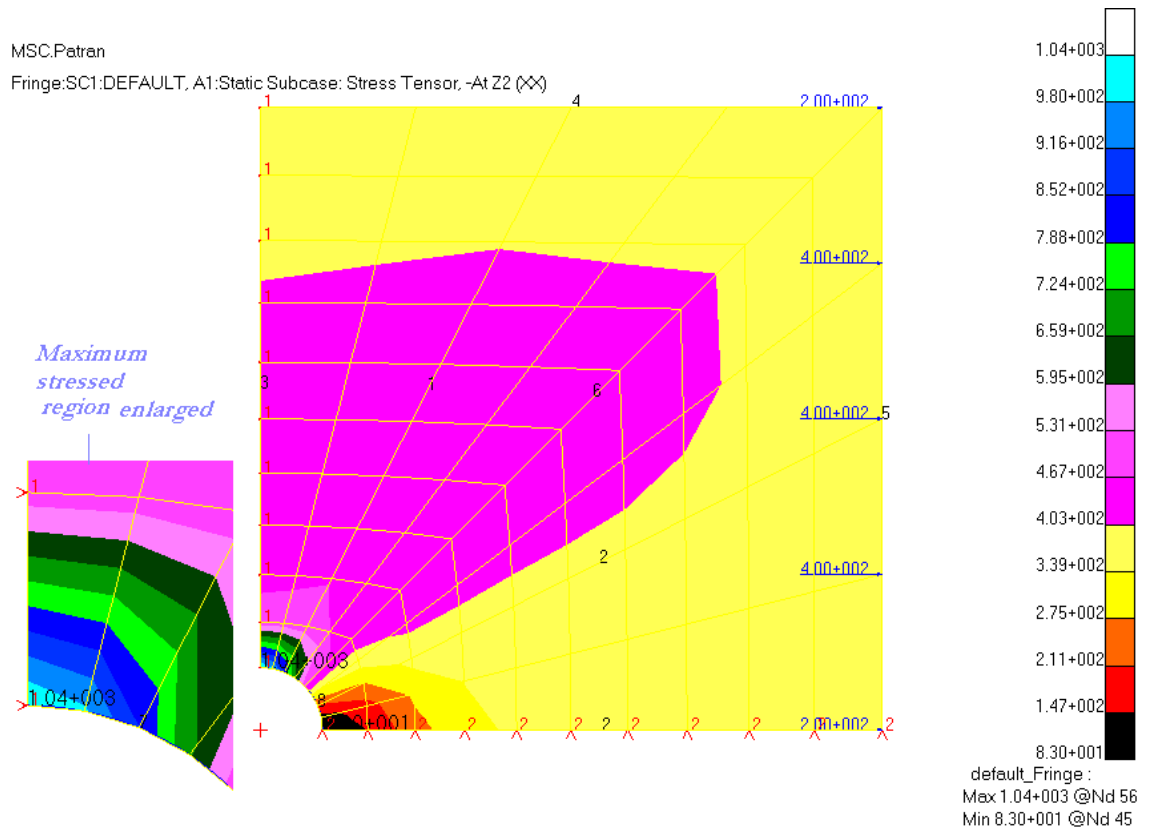


Fig 4.7 Result of model 2

The result file is shown in Fig 4.7. From the figure it is seen that the maximum stress developed is 1040 psi. So the stress concentration factor is $1040/400 = 2.6$.

4.2.3.3 Model 3

Since the mesh quality of the elements near the hole is not satisfactory in Model 2 and also we know that the stress concentration occurs at that region, we are intended to refine our mesh. For this reason, in our next model we rearrange mesh seeds though the number of nodes and elements are same as Model 2. The next model has mesh seed as Fig 4.8.

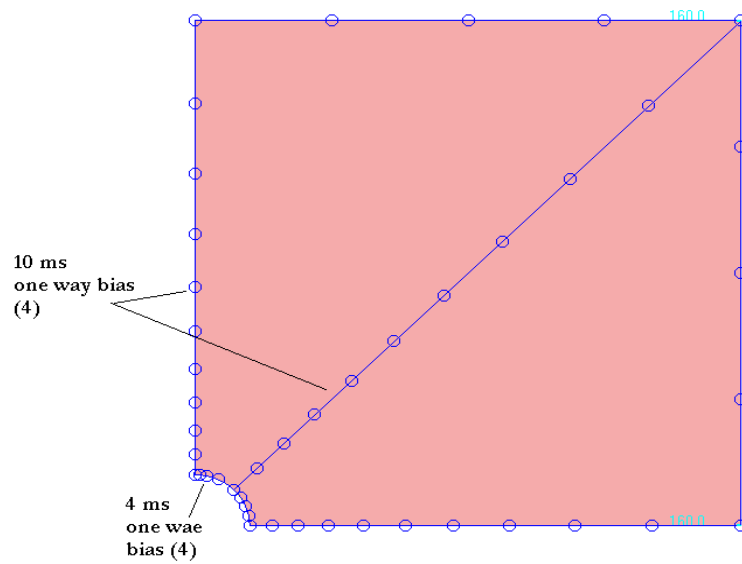
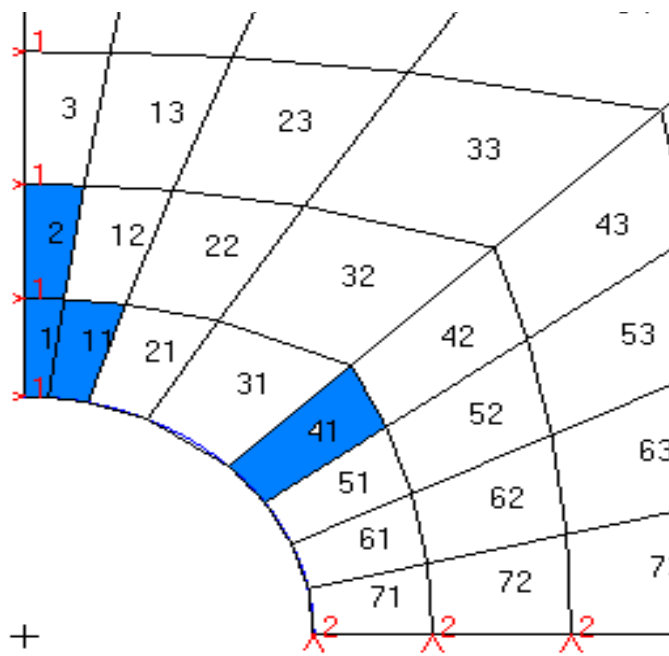
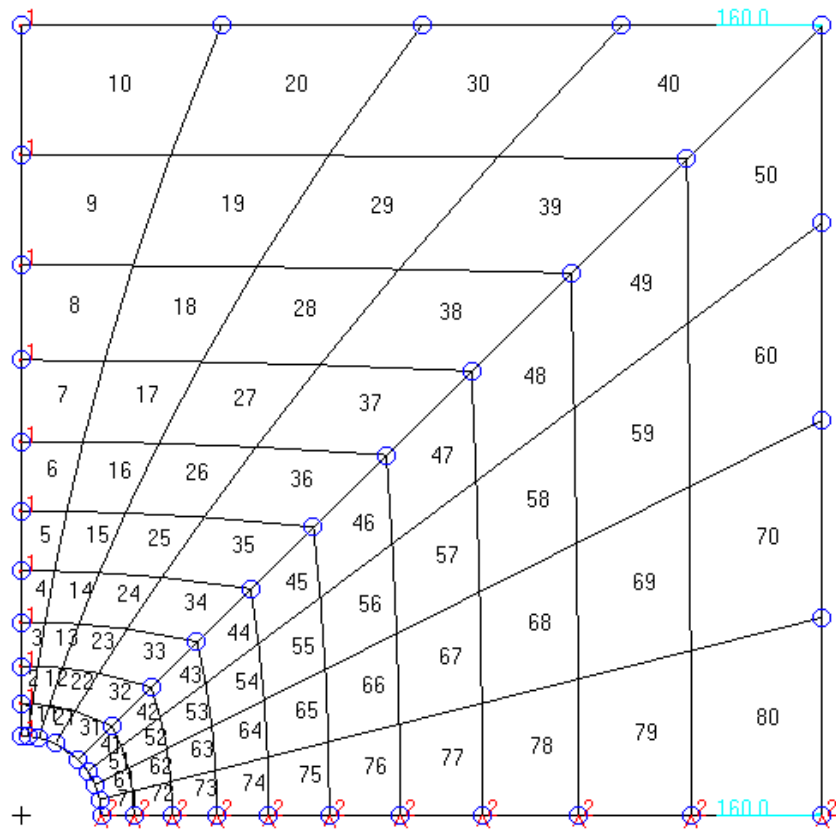


Fig 4.8 Mesh seed for model 3



Enlarged around the maximum stressed region

Fig 4.9 Mesh for model 3

The mesh of model 3 is shown in Fig 4.9. The model has 99 nodes and 80 quadrilateral elements. The output(in short form) of MESH QUALITY_2012 for model 3 is as follows:

quad no	angle1	angle2	angle3	angle4	distortion factor	aspect ratio
1	92.470327	88.620336	83.890044	95.019292	8.398265	4.786649
2	91.379664	89.146234	82.573480	96.900623	10.266654	3.444965
3	90.853766	89.427968	81.373599	98.344667	12.045929	2.692061
4	90.572032	89.575413	80.160324	99.692231	13.829897	2.201760
.
.
.
10	90.159768	90.000000	68.942715	110.897517	29.667170	1.528809
11	91.373477	91.907360	77.836832	98.882331	15.243455	3.142946
12	87.301974	94.450396	74.966787	103.280844	20.723505	2.364000
14	82.502873	98.204482	70.436370	108.856275	29.356689	1.659506
15	80.560804	99.941172	68.251745	111.246279	33.351406	1.470690
16	78.630958	101.752363	65.960516	113.656163	37.481783	1.332436
17	76.601633	103.714667	63.495178	116.188521	41.904088	1.280963
20	69.231945	111.057285	54.747461	124.963309	57.791832	1.422186
21	91.265202	95.674429	71.246864	101.813505	22.913728	2.210756
25	70.982076	110.183792	58.401349	120.432784	51.900829	1.256935
30	55.166484	125.252539	47.091718	132.489258	78.118967	1.237005
31	94.293792	98.570164	67.253972	99.882072	26.587996	1.739232
32	80.638420	106.656245	59.959307	112.746028	42.248014	1.409693
38	53.130873	127.847616	46.303578	132.717933	80.783499	1.370878
39	50.353223	130.401692	45.548663	133.696422	84.198945	1.254248
40	47.640382	132.908282	45.000000	134.451337	87.386379	1.099186
41	95.625150	69.918354	102.199042	92.257454	24.265769	3.045180
42	110.081646	61.622793	110.501877	77.793684	42.164671	2.450516
43	118.377207	56.463412	115.668686	69.490695	54.858743	2.039004
50	134.443217	45.000000	127.127070	53.429713	81.951234	1.205053
51	98.992816	70.529051	99.302348	91.175785	23.407365	2.670724
71	98.722095	78.944659	86.708712	95.624533	15.516554	2.162934
72	101.051686	77.741517	87.915509	93.291288	16.958416	1.643811
73	102.254821	77.043112	88.617576	92.084491	18.008825	1.362208
74	102.953333	76.615114	89.049129	91.382424	18.701852	1.293904
75	103.381640	76.346215	89.321274	90.950871	19.153563	1.264763

76	103.651463	76.173576	89.496235	90.678726	19.448570	1.303394
77	103.824661	76.054007	89.617567	90.503765	19.647189	1.372908
78	103.947680	75.951787	89.718100	90.382433	19.801914	1.432571
79	104.051863	75.833416	89.832821	90.281900	19.956311	1.484023
80	104.176088	75.656733	90.000000	90.167179	20.167268	1.528809

*****bad quadfaces, distortion factor more than 105(the passing mark).*****

*****average distortion factor and aspect ratio*****

43.483030 1.654446

*****quad with worst distortion factor*****

40, 87.386379

*****quad with worst aspect ratio*****

1, 4.786649

From Fig 4.9 we see that only four members (fewer than Model 2) have aspect ratio larger than three and those are shown as by coloring.

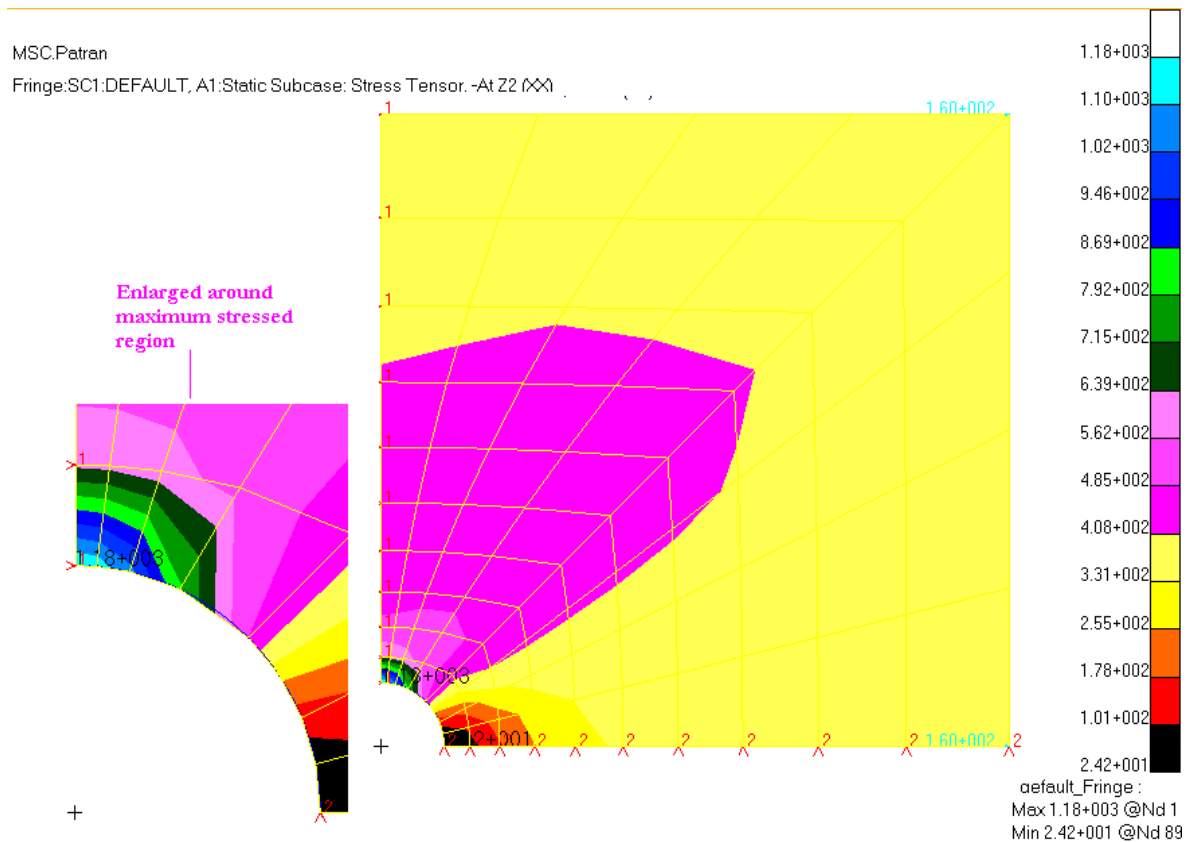


Fig 4.10 Result of model 3

The result file is shown in Fig 4.10. From the figure it is seen that the maximum stress developed is 1180 psi. So the stress concentration factor is $1180/400 = 2.95$.

4.2.3.4 Model 4

The mesh remaining same (same seeding as in Fig 4.8) as model 3 but the elements near the hole are subdivided (along the larger length of the elements) to modify the aspect ratios. As a result, the number of nodes in the next model (Model 4) becomes 117 and the number of element is 96. The Model 4 has mesh seed as Fig 4.11.

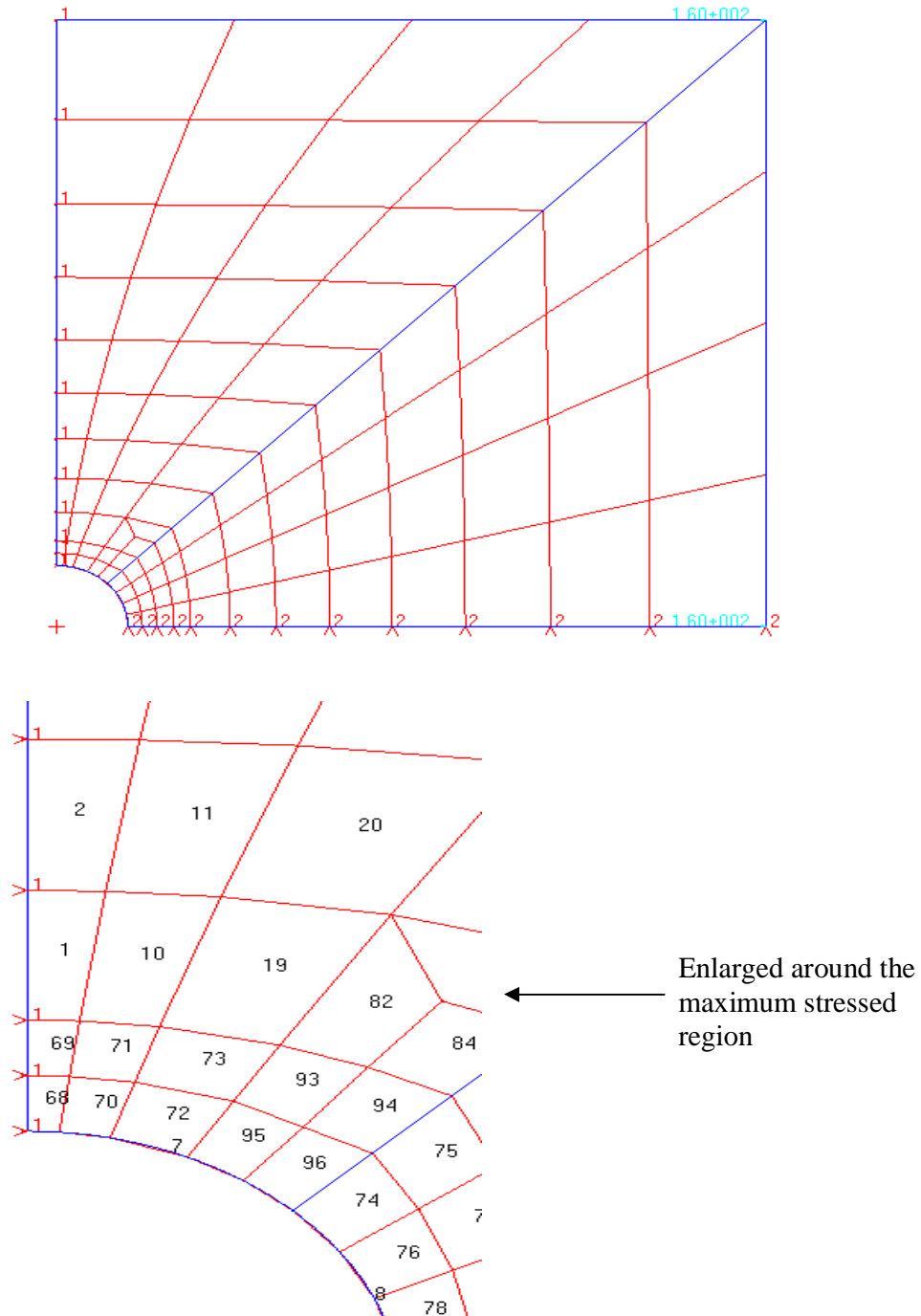


Fig 4.11 Mesh of model 4

The output (in short form) of MESH QUALITY_2012 for model 4 is as follows, where the elements near the hole have mentioned.

quad no	angle1	angle2	angle3	angle4	distortion factor	aspect ratio
1	91.379664	89.146234	82.573480	96.900623	10.266654	3.444965
.
.
.
67	104.176088	75.656733	90.000000	90.167179	20.167268	1.528809
68	92.470327	88.200210	84.324828	95.004635	8.160620	2.393221
69	91.799790	88.620336	83.875388	95.704486	8.671490	1.825570
70	91.388135	90.612760	79.116323	98.882783	14.130133	1.571446
71	89.357927	91.922016	77.837284	100.882773	16.446058	1.227760
72	91.264750	92.907620	74.005782	101.821848	20.140133	1.262864
73	87.093284	95.673977	71.255207	105.977532	25.441930	1.520861
74	95.625150	75.823249	96.292885	92.258716	16.653071	1.522572
75	104.176751	69.918354	102.200304	83.704591	28.155504	1.252773
76	98.991555	74.737866	95.094594	91.175985	18.469397	1.335557
77	105.264658	70.527789	99.302548	84.905004	26.919754	1.259897
78	100.073939	76.046231	91.352722	92.527107	17.447293	1.257658
79	103.954170	73.496656	93.900056	88.649118	22.002604	1.405004
88	112.886911	64.683592	105.143867	77.285630	39.442656	1.518324
89	106.507068	71.452605	95.938372	86.101955	25.825340	1.448806
90	108.548910	70.003047	97.384970	84.063073	28.874298	1.694643
91	101.052409	78.234240	87.422064	93.291288	16.675346	1.517006
92	101.764316	77.742239	87.915509	92.577936	17.310190	1.773281
93	86.709901	101.695891	71.170121	100.424087	24.715269	1.346872
94	79.572157	102.555810	70.393970	107.478063	30.923574	1.434902
95	89.345421	93.306785	78.631388	98.716407	14.716806	1.464165
96	91.165645	101.372369	72.521937	94.940049	21.461041	1.733098

*****bad quadfaces, distortion factor more than 105(the passing mark).*****

*****average distortion factor and aspect ratio*****

40.684585 1.498629

*****quad with worst distortion factor*****

35, 87.386379

*****quad with worst aspect ratio*****

1, 3.444965

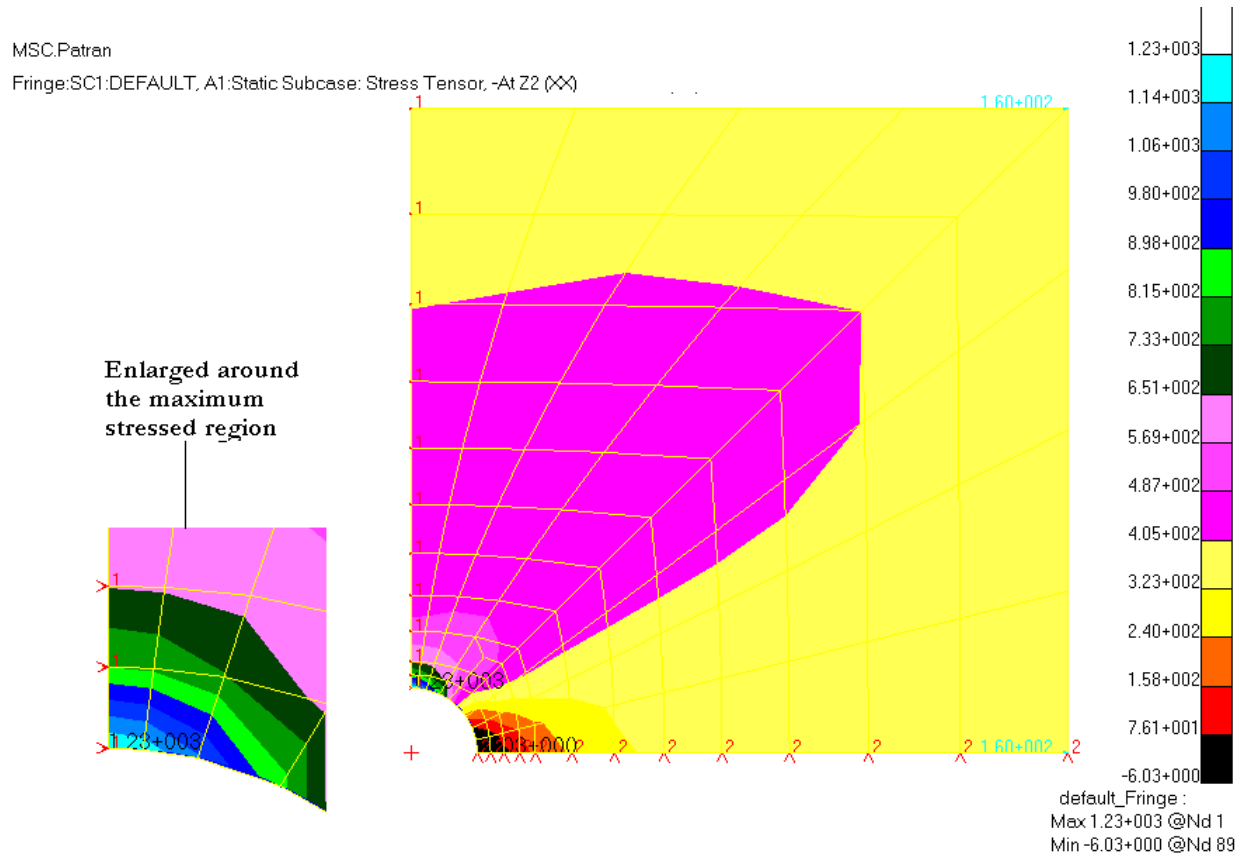


Fig 4.12 Result of model 4

The result is shown in Fig 4.12. From the figure it is seen that the maximum stress developed is 1040 psi. So the stress concentration factor is $1230/400 = 3.075$.

So we now summarize the results in table below.

Model No.	No. of Nodes	No. of Elements	Applied In-plane stress, σ (psi)	Maximum stress developed, σ_{max} (psi)	Average Df^I	Average AR^2	Maximum AR	No of AR more than 3	Numerical K_{lg}	Theoretical K_{lg}	% difference
1	27	16	400	589	46.930	17.21	33.52	16	1.4725	3.0354	51.49
2	99	80	400	1040	46.070	2.06	5.43	9	2.6	3.0354	14.345
3	99	80	400	1180	43.480	1.65	4.80	4	2.95	3.0354	2.8
4	117	96	400	1230	40.685	1.50	3.44	1	3.075	3.0354	1.3

DF = Distortion factor; AR = Aspect ratio

Table 4.1. Summary of models and their out put

From Table 4.1 we see that the desired correct result does not depend on the increasing number of nodes and elements. With same number of nodes and elements, model 3 gives better results than model 2. As the models have better quality (in terms of distortion factor and aspect ratio), we approach to the desired result.

4.2.4 Finite Element Analysis of a Plate with a center hole and additional holes in a plane perpendicular to the loading direction

After finding out the correct approach to mesh a model, our next problem which is not listed in Pilkey & Pilkey (2008) is a plate with a center hole and two additional smaller holes. We placed the additional holes to see the effect of stress concentration in the region where originally the maximum stress developed.

The schematic diagram is as follows:

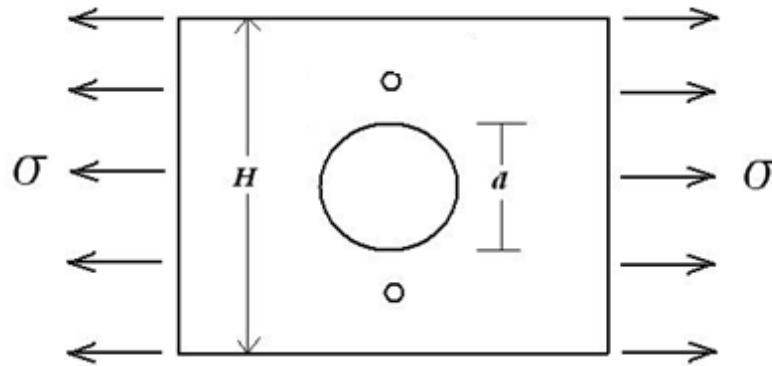


Fig. 4.13 A plate with a center hole and additional holes in a plane perpendicular to the loading direction

For modeling and analysis we placed an additional hole of 0.5 inch diameter (in the quarter mode) and placed its centre 5.5 inch away from the centre of the central hole (remaining length above center hole/2 = $9/2 = 4.5$). All other dimensions and parameters are kept same.

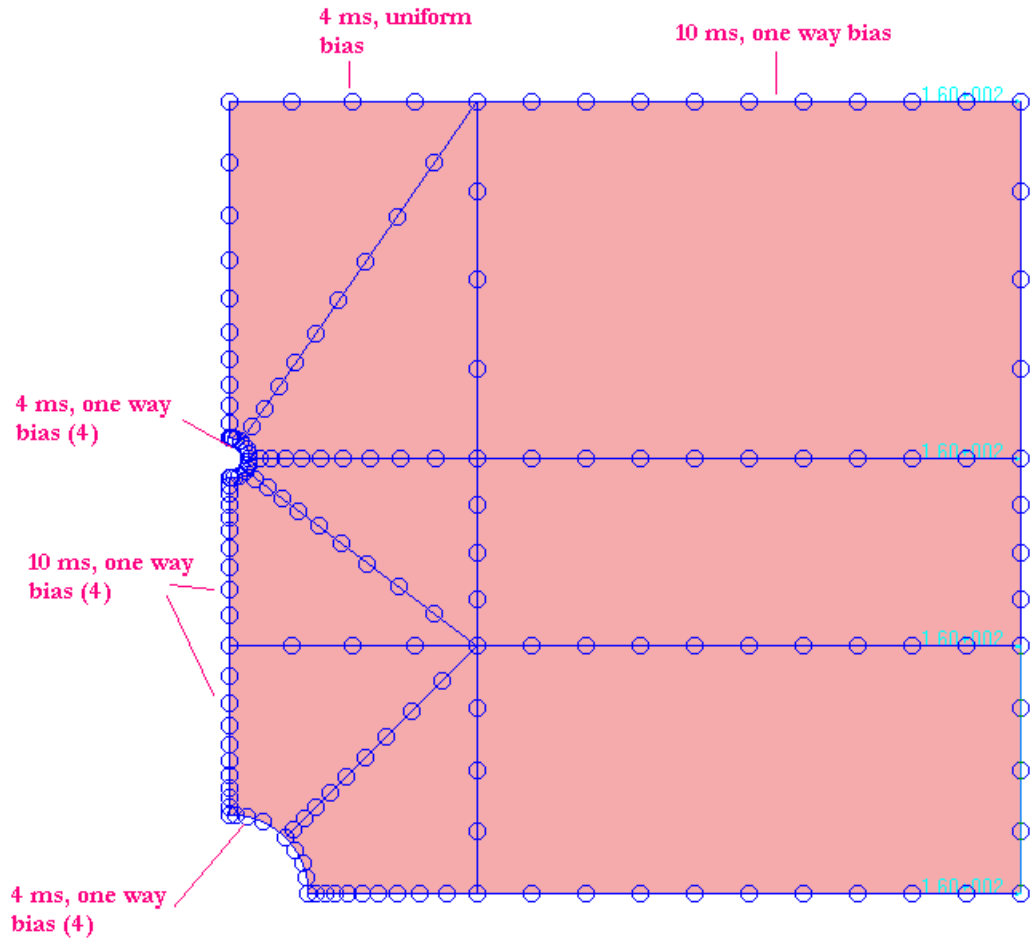


Fig 4.14 Mesh seed for model with additional hole

The generated mesh is shown in Fig 4.15. It is to be noted here that the elements of higher aspect ratio are refined.

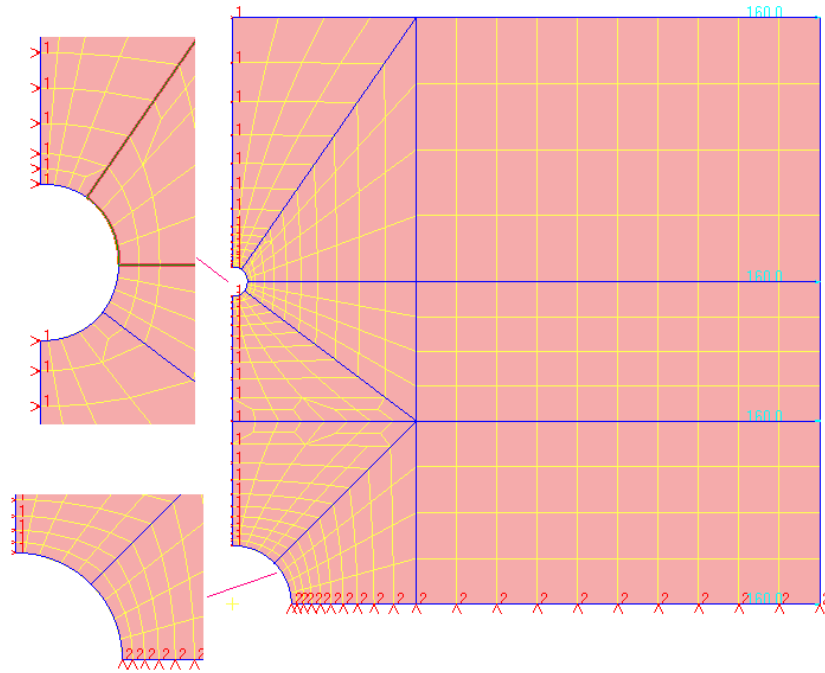


Fig 4.15 Mesh of model with additional hole

The out put of is as follows:

quad no	angle1	angle2	angle3	angle4	Distortion factor	aspect ratio
1	90.294859	89.785437	83.535635	96.384068	9.092707	3.780323
2	90.214563	89.819493	82.600617	97.365327	10.444019	3.068710
5	90.142921	89.880192	78.862612	101.114275	15.735415	1.850013
.
.
.
318	90.000000	90.000000	90.000000	90.000000	0.000000	1.639156
319	90.000000	90.000000	90.000000	90.000000	0.000000	1.639142
320	90.000000	90.000000	90.000000	90.000000	0.000000	1.639142
321	91.061526	89.220006	86.111848	93.606620	5.464491	3.738455
364	98.695380	135.058930	45.000000	81.245691	64.865667	2.220641
366	141.449409	38.835041	59.525175	120.190376	84.291569	3.201113
367	142.286432	97.772947	82.790698	37.149923	75.095900	2.843970
368	157.692488	41.740039	134.230696	26.336777	113.669069	1.847521
371	47.867549	152.627368	30.823862	128.681222	103.418484	2.043926

372	44.898436	134.449206	48.519907	132.132451	86.635008	1.000000
373	45.549424	133.806136	21.791714	158.852726	115.273151	2.318610
374	134.414335	75.172364	90.000000	60.413301	55.388309	1.952721
397	83.318721	97.689750	72.454628	106.536901	26.174051	1.209095
398	128.032539	48.481859	128.016029	55.469573	76.208916	2.109067
399	131.520163	45.134833	84.397165	98.947839	62.034367	2.344328
400	127.307935	133.036132	42.854086	56.801846	81.048413	3.524343
401	119.413689	56.316775	136.572634	47.696902	77.189941	2.480238
402	123.683225	51.965082	124.529943	59.821751	68.441642	2.191283
403	163.605615	52.692549	123.197522	20.504314	112.877625	3.024109
415	116.775089	75.260045	106.315111	61.649754	44.767075	1.590135
416	118.348223	73.686069	107.451309	60.514399	47.367869	1.847080

*****bad quadfaces, distortion factor more than 105(the passing mark).*****

368 113.669069

369 123.092536

373 115.273151

403 112.877625

*****average distortion factor and aspect ratio*****

31.843396 1.555439

*****quad with worst distortion factor*****

369, 123.092536

*****quad with worst aspect ratio*****

107, 3.922250

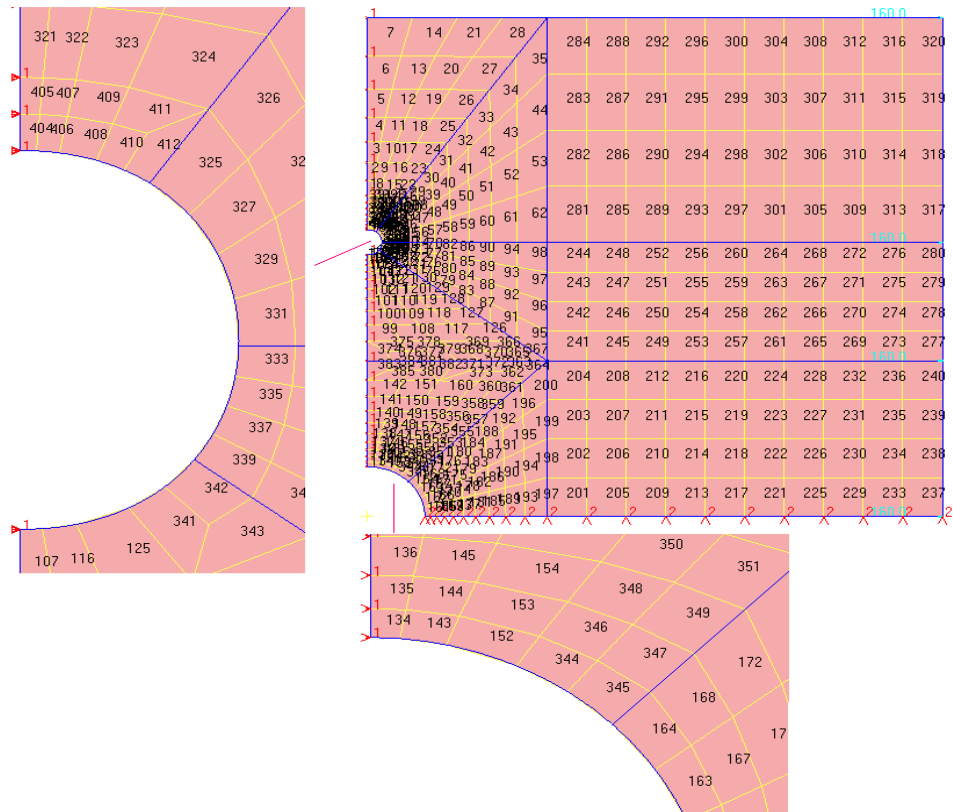


Fig 4.16 Mesh of model (with element numbers) with additional hole

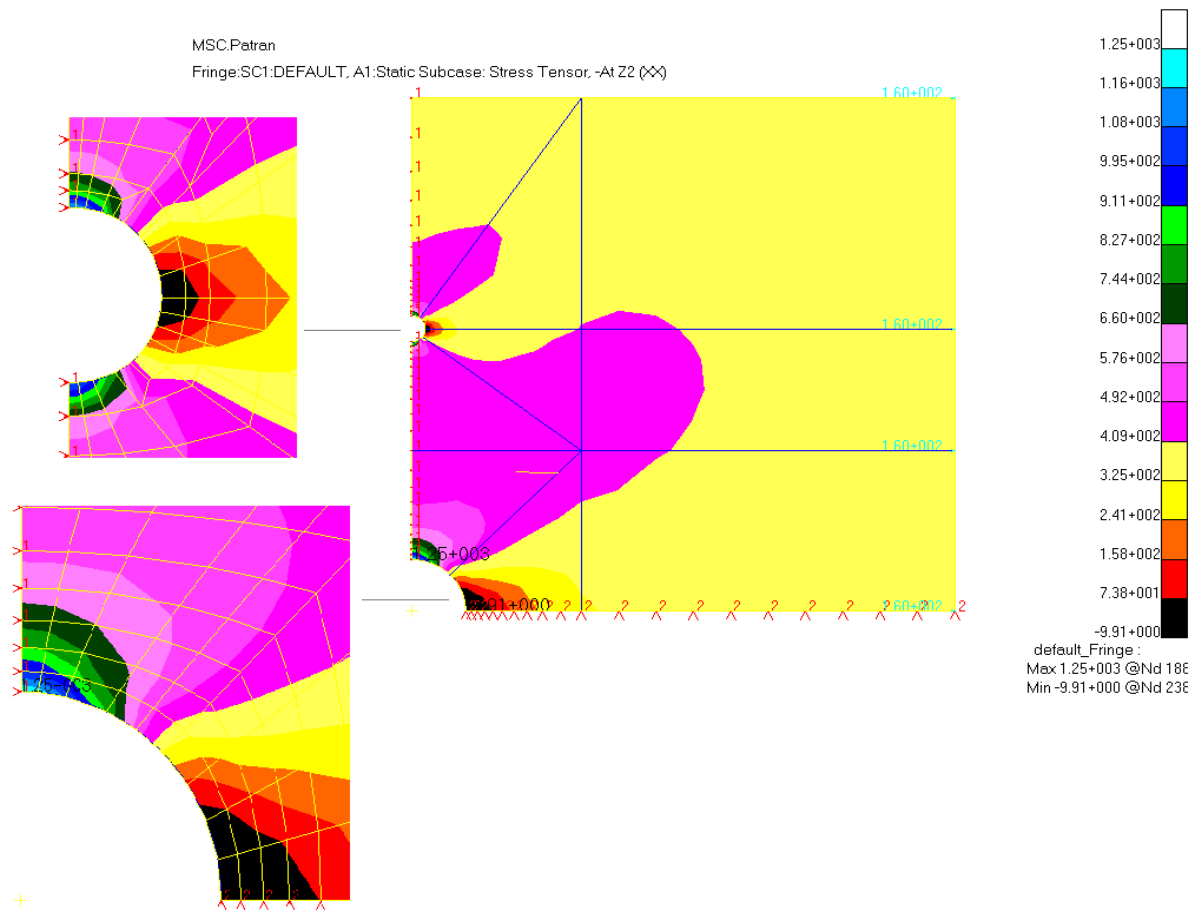


Fig 4.17 Result of model with additional hole

The result is shown in Fig 4.17. From the figure it is seen that the maximum stress developed is 1250 psi. So the stress concentration factor is $1250/400 = 3.125$ (more than 3.075, the stress concentration found from previous problem). So we see that the addition of holes will not make the situation better but will worsen the case. Now we get two additional regions with stress concentration (extreme edges of the smaller hole).

4.2.5. Verification of the Infiniteness of the Model

The formulation of the physical model in section 4.2 involves the plate to be infinite in length. When the hole is sufficiently far away from the lateral edge of the plate, the model is to be considered as infinite in length. At this stage of the analysis the plate is to be considered as of finite length. For this purpose a finite element model is being created using hole of 2 inch diameter (d) and the plate of length (A) 10 inch. Width (H) of the plate is taken as 20 inch. All other dimensions and parameter are kept same. The generated mesh is shown in the following figure.

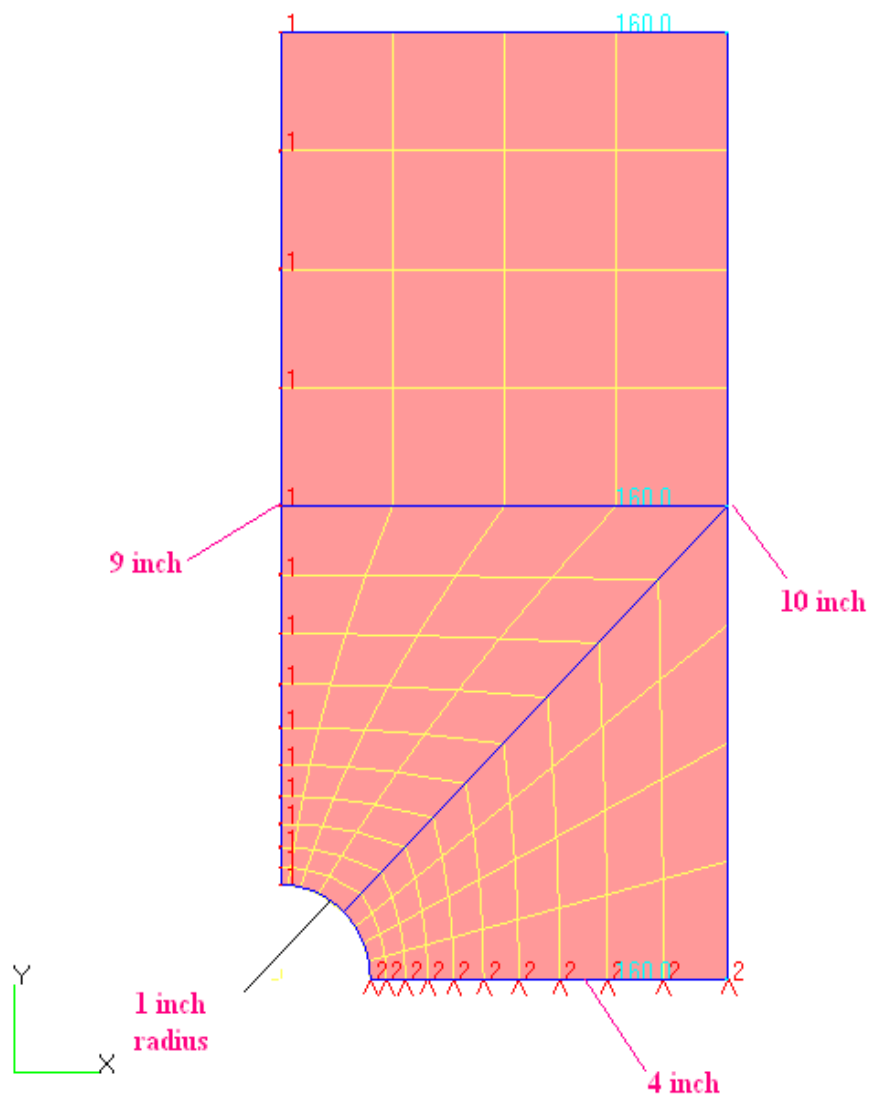


Fig. 4.18 .Plate (finite length) with hole

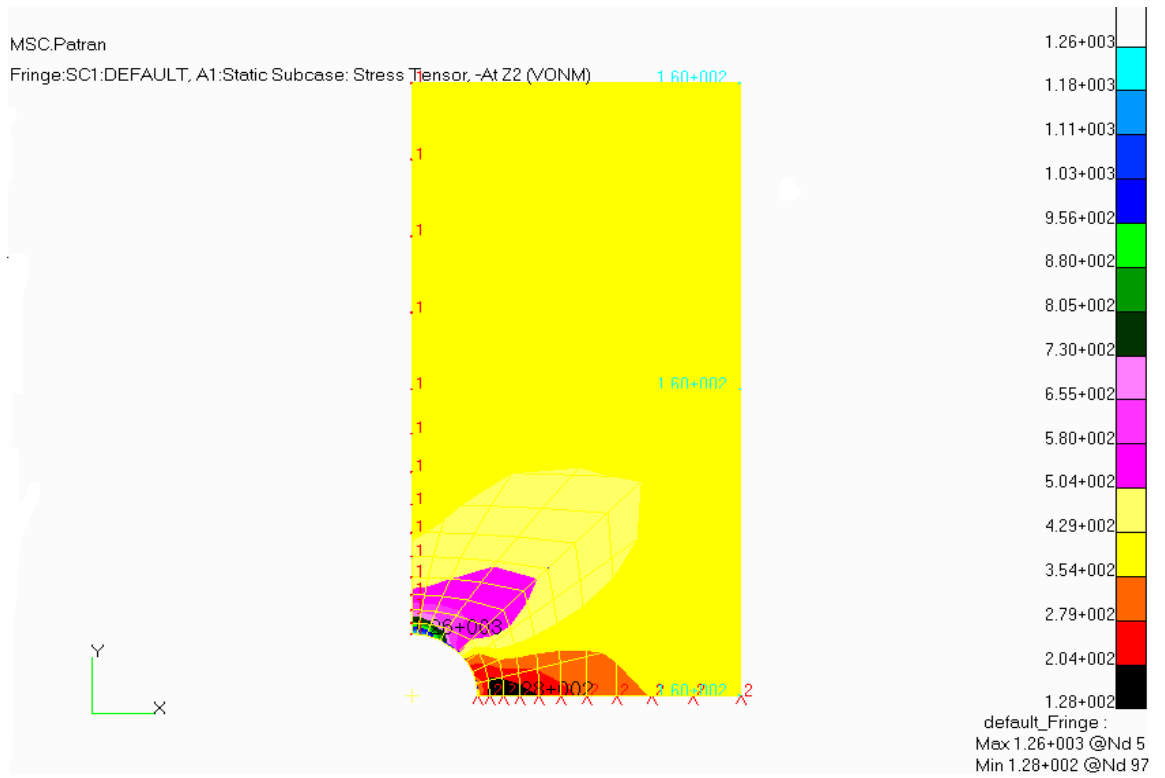


Fig 4.19 Plate (finite length) with hole (Von Mises stress)

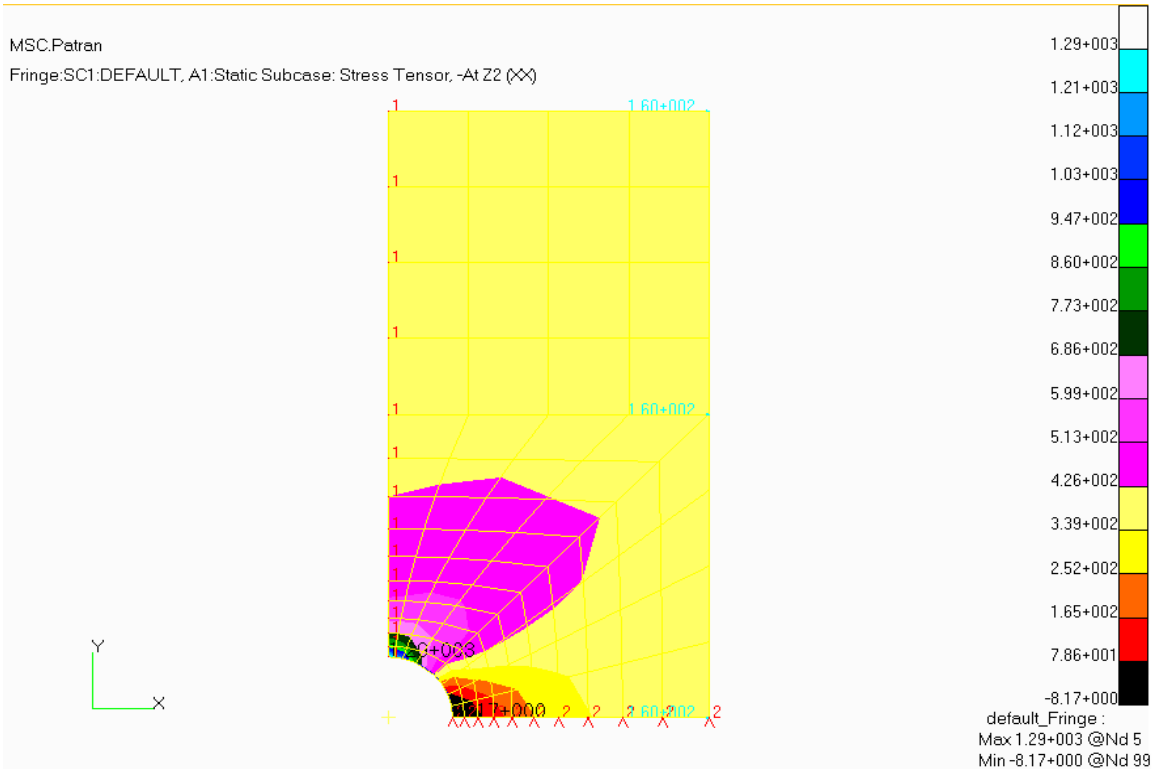


Fig 4.20 Plate (finite length) with hole Maximum stress (X Component)

From the figures 4.19 and 4.20 it is seen that the maximum stress developed is 1290 psi (in X component) and is 1260 psi (von mises). For the obvious reasons the maximum stress increased to 1260-1290 psi for finite plate from the range of 1190-1230 psi for infinite plate.

4.2.6. Von Mises Stress

In this section the results are shown (for all models) in terms of Von Mises stress. Von Mises stress is a geometrical combination of all the stresses (normal stress in the three directions, and all three shear stresses) acting at a particular location. Since it is a stress, it is measured in Pascal, just like any other type. Von Mises stress is useful for materials which classify as ductile. If the Von Mises stress at a particular location exceeds the yield strength, the material yields at that location. If the Von Mises stress exceeds the ultimate strength, the material ruptures at that location. The failure criterion states that the Von Mises stress S_{VM} should be less than the yield stress S_Y of the material. In the inequality form, the criterion may be put as

$$S_{VM} \leq S_Y$$

The Von Mises stress S_{VM} is given by

$$S_{VM} = \sqrt{I_1^2 - 3I_2}$$

where I_1 and I_2 are given by

$$I_1 = S_x + S_y + S_z$$

$$I_2 = S_x S_y + S_y S_z + S_z S_x - t_{yz}^2 - t_{xz}^2 - t_{xy}^2$$

MSC.Patran

Fringe:Default, A1:Static Subcase: Stress Tensor, -At Z2 (VONM)

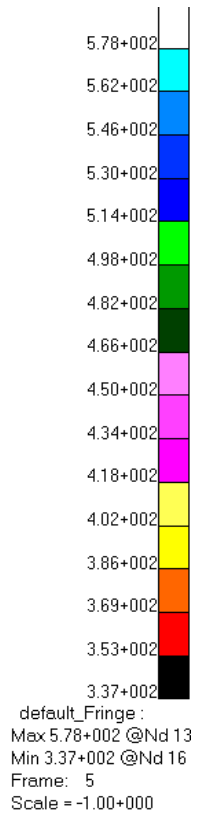
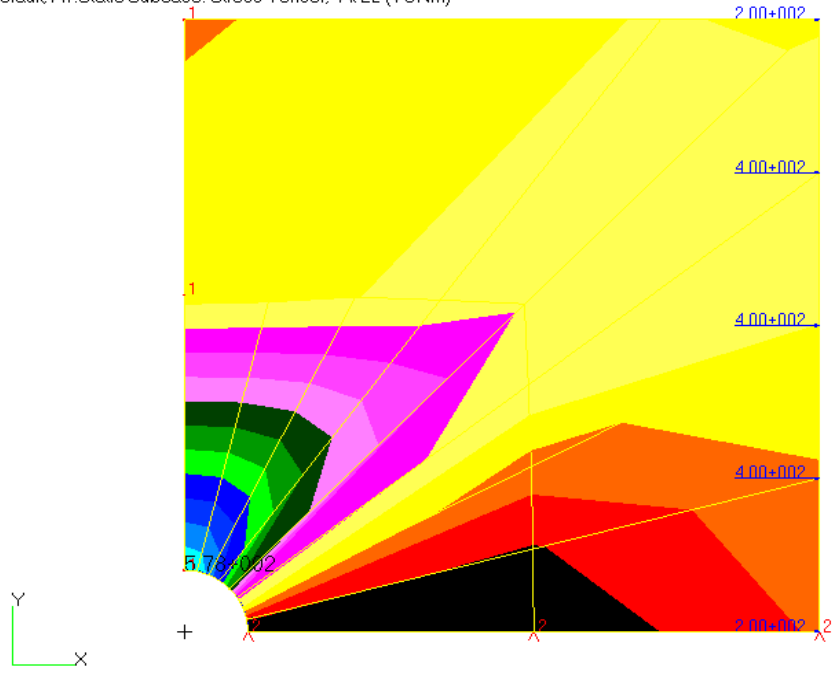


Fig.4.21 Von mises stress for model 1

MSC.Patran 12.0.041 06-Jan-06 01:31:44

Fringe:SC1:DEFAULT, A1:Static Subcase: Stress Tensor, -At Z2 (VONM)

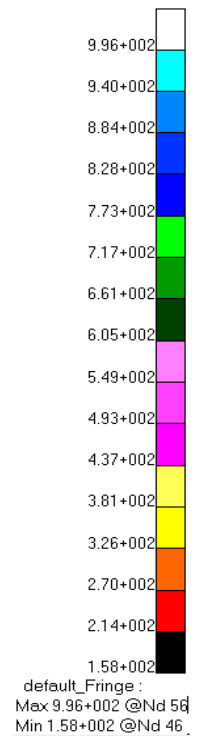
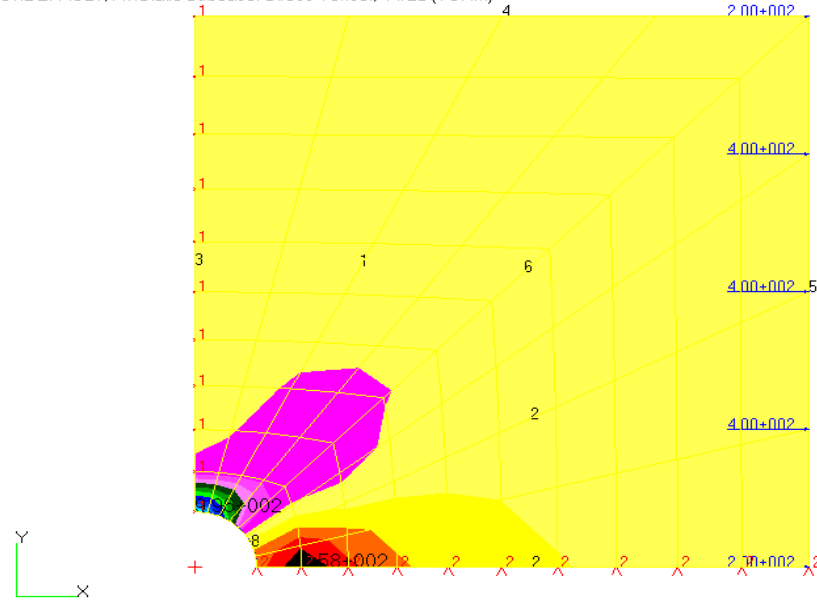


Fig. 4.22 Von mises stress for model 2

MSC.Patran 12.0.041 06-Jan-06 01:29:53
 Fringe:Default, A1:Static Subcase: Stress Tensor, -At Z2 (VONM)

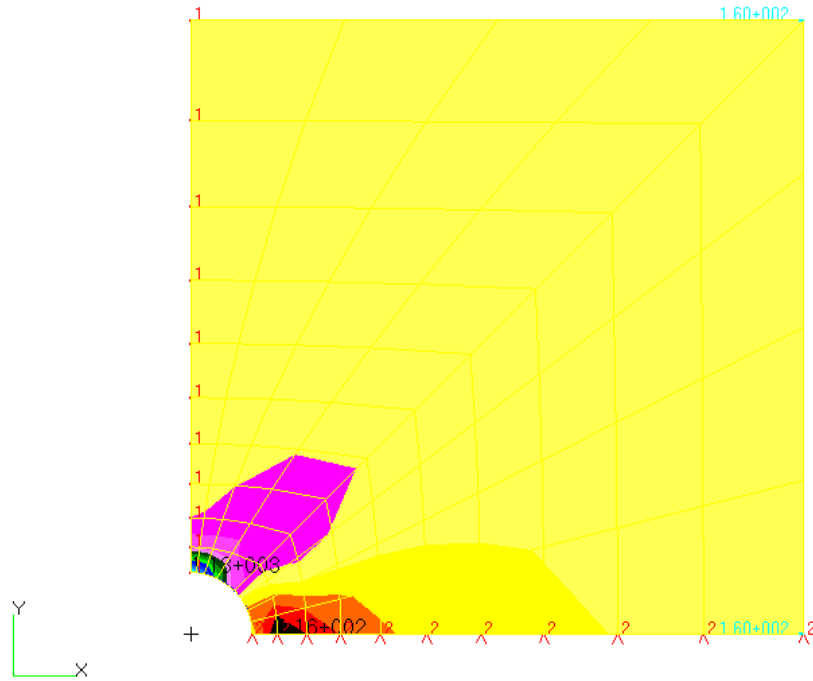


Fig.4.23 Von mises stress for model 3

MSC.Patran
 Fringe:SC1:DEFAULT, A1:Static Subcase: Stress Tensor, -At Z2 (VONM)

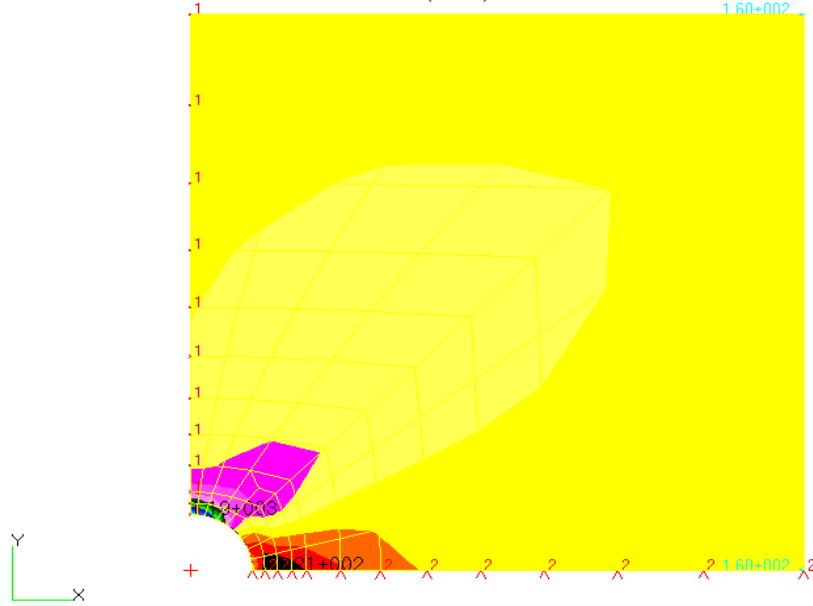


Fig. 4.24 Von mises stress for model 4

MSC.Patran 12.0.041 06-Jan-06 02:10:02
 Fringe:SC1:DEFAULT, A1:Static Subcase: Stress Tensor, -At Z2 (VONM)

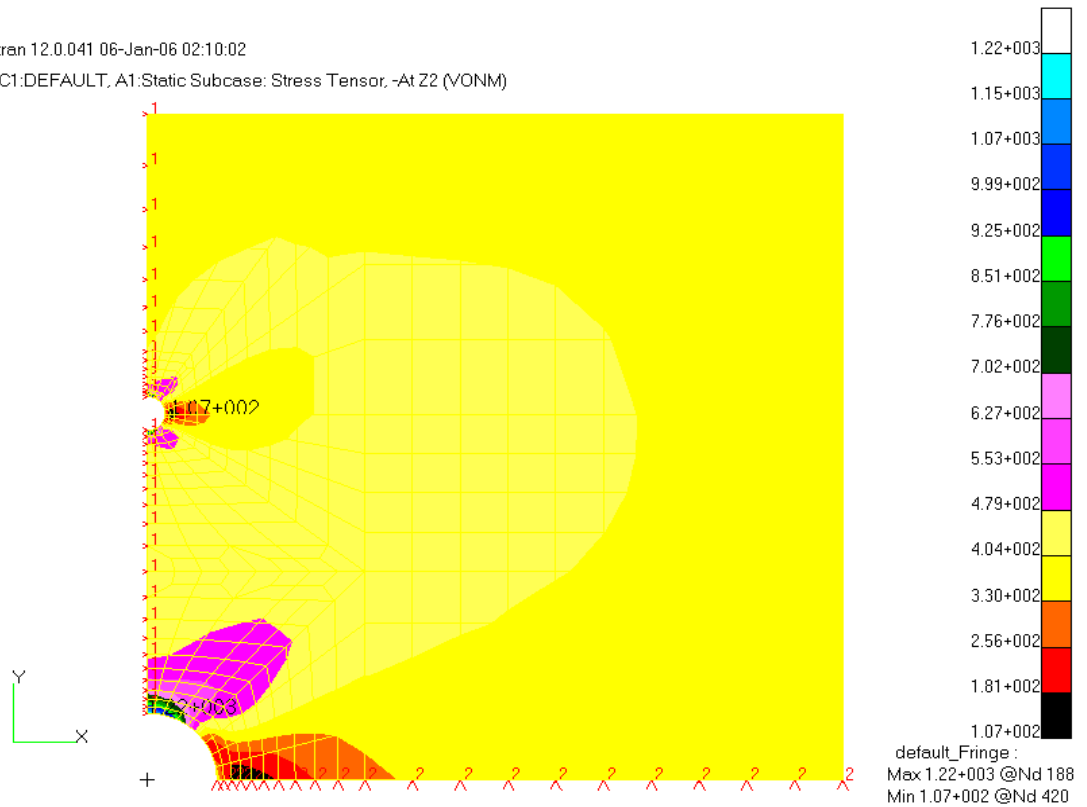


Fig. 4.25 Von mises stress for model with additional hole

So we now summarize the results in the following table.

Model	S_{max} (Maximum Von Misses stress)	S (Von Mises stress at the edge nodes where pressure applied)	K_{tg} (Numerical)	K_{tg} (theoretical)	% difference
1	578.00	400	1.445	3.0354	52.40
2	996.00	400	2.490	3.0354	17.97
3	1130.0	400	2.825	3.0354	6.900
4	1190.0	400	2.975	3.0354	1.990
5 (Finite model)	1260.0	400	3.150	3.0354	3.780
6 (Additional hole)	1220.0	400	3.050	Unknown	0.480*

* With respect to the K_{tg} of column 5

Table 4.2 Stress concentration factor in terms of Von Mises stress

CHAPTER 5

CONCLUSIONS AND RECOMMENDATION

5.1 Conclusions

In this study the main target was to perform a FEM analysis on a structural problem concerning stress concentration around a hole in the middle of an infinitely long plate to validate the formula for the problem and by this to find out correct meshing of the domain. The high stress concentration found at the edge of a hole is of great practical importance. As an example, holes in ships' decks may be mentioned. When the hull of a ship is bent, tension or compression is produced in decks and there is a high stress concentration at the holes. Under the cycles of stress produced by waves, fatigue of the metal at the overstressed portions may result finally in fatigue cracks. Also in the aviation industry, the localized stress distribution concept forms a very useful aspect in the building of aircrafts, where the discontinuities in plates are quite commonly encountered in the construction of windows, frames etc of the aero-planes.

The following conclusions can be drawn from the present study:

1. A reliable program in c++ is developed which can effectively check the quality of 2-dimensional quadrilateral finite element mesh. To achieve correct result a good quality mesh is necessary and for evaluating if the mesh is good enough, this program is very much essential.
2. After performing a number of investigations (only four are given in section 4.2.3) a reliable meshing technique is proposed (Section 4.2.4), using which a mesh consisting of a minimum number of elements can be generated for achieving accurate results.
3. It is found from the analyses that element aspect ratio has a great impact on the finite element results. The maximum allowable aspect ratio (the best is 1) is found to be 3.44. But care should be given to keep elements having higher

aspect ratio away from region of high stress concentration and numbers of these elements to be minimum.

4. Though the distortion factor of value zero means perfect square (the best possible), but for geometric constraints achieving this value is not always possible. From the analyses we made, it is found that the average distortion factor of the mesh should not be more than 40.
5. After investigating the results obtained in Section 4.2.3 the formula (equation 4.1) given by Pilkey & Pilkey (2008) is found reasonably accurate.
6. The proposed meshing technique is used for a plate with center hole and additional holes in a plane perpendicular to the loading direction. It is seen that the presence in additional hole increases the stress concentration factor in the original place and moreover two additional points are found to have stress concentration. Thus the effect of additional hole is very detrimental.
7. The proposed meshing technique can be extended to a plate having any number of holes.

5.2 Recommendation for Further Study

This thesis provides a strong foundation for further study on this subject. This study recommends the following topics as possibilities for future work:

1. Finite element modeling of structures having cracks:

All of the finite element models used in this thesis have been made for structures having hole. However, structure having crack is also a very important topic. Study for achieving correct meshing for this problem will be valuable to a finite element analyst.

2. Finite element modeling of structural discontinuities in more complex structures:

The finite element models that we have considered in this study are for plate structures. However, future research groups may investigate the possibility of using finite elements to study the behavior of structural discontinuities in three-dimensional structures.

3. Adaptation of user friendly software:

To see the effects of varying the position of holes in structures, we had to manually reconfigure the model for each case, which was very tedious. However, future research groups may contribute to create more user friendly software where the mesh generation process will be trouble-free. In other words more advanced automatic mesh generation program should be developed. A considerable progress in this field is already achieved.

REFERENCES

- Alblas, J.B.: Theorie van de Driedimensionale Spanning Stoestand in een Doorboorde Plat, Dissertation, Delft 1957.
- Allam, M. N. M., ZenKour, A. M., “Stress concentration factor of a structurally anisotropic composite plate weakened by an oval opening”, *Composite Structures*, vol. 61, pp. 199–211, 2003.
- Baker, Timothy, J., “Automatic Mesh Generation for Complex Three-Dimensional Regions Using a Constrained Delaunay Triangulation”, *Engineering with Computers*, vol. 5, pp. 161-175, 1989.
- Brauer, J.R., ed., *What Every Engineer Should Know About Finite Element Analysis*, Marcel Decker Inc., 1993.
- Chai, B.G., “Free vibration of laminated plates with a central circular hole”, *Compos Struct*, vol. 35, pp. 357–68, 1996.
- Chaudhuri, R. A., “Stress concentration around a part through hole weakening laminated plate”, *Computers and Structures*, Vol. 27, No 5, pp. 601-609, 1987.
- Daoust, J., Hoa, S.V., “An analytical solution for anisotropic plates containing triangular holes”, *Compos Struct.*, vol. 19, pp.107–30, 1991.
- Delale, F., Kishore, N.M. and Wang, A. S. D., “Stress Analysis of a composite plate with a circular hole under axisymmetric bending”, *J. Camp. Maler*, vol. 18, pp. 420, 1984
- Folias, ES., WangJJ., “ On the 3-dimensionl stress field around a circular holes in a plate of arbitrary thickness”, *Comput Mech*, vol. 6(3), pp. 379–91, 1990.
- Fraser, W.B., “Bending of a highly stretched plate containing an eccentricly plate-reinforced circular hole”, *Int. J. Solids Swucr*, vol.11, SO1, 1975.
- George, P. L., Hecht, F. and Saltel, E., “Automatic Mesh Generator with Specified Boundary”, *Computer Methods in Applied Mechanics and Engineering North-Holland*, vol. 92, pp. 269-288, 1991.
- Huang, M. and Sakiyama T., “Free vibration analysis of rectangular plates with variously shape-holes”, *J Sound Vib*, vol.226, pp.769–86, 1999.
- Hughes, T.R.J., *The Finite Element Method*, Prentice Hall, Englewood Cliffs, N.J.,1987.
- Islam, M.S., Rahman, N.I. and Uddin, M.M., “A Practical Approach to Triangulation of Planar Surface”, *The International Conference on Marine Technology, Proceedings of MARTEC*, 2010.

Iwaki, T., "Stress concentrations in a plate with two unequal circular holes," *International Journal of Engineering Sciences* vol. 18 (8), pp. 1077–1090, 1980.

Jain, N. K., Mittal, N. D., "Finite element analysis for stress concentration and deflection in isotropic, orthotropic and laminated composite plates with central circular hole under transverse static loading", *Materials Science and Engineering*, vol. A 498, pp. 115–124, 2008.

Ko, W., "Stress concentration around a small circular hole in the Hi-Mat composite plates", NASA TM 86038, 1985.

Lekhnitskii, S.G. *Theory of elasticity of an anisotropic body*, Moscow, Mir Publishers; 1961.

Lekhnetski, S.G., *Anisotropic flares* (Translated by S. W. Tsai and T. Cheron), pp. 394-419, Gordon & Breach, New York, 1968.

Lawson, C. L., "Software for CI Surface Interpolation", *Mathematical Software III*, pp. 161-194, 1977.

Lo, S.H., "A new mesh generation scheme for arbitrary planar domains", *International Journal for Numerical Methods in Engineering*, vol. 21(8), pp.1403-1426, 1985.

Lo, S. H. and Lee, C. K., "On using meshes of mixed element types in adaptive finite element analysis", *Finite Elements in Analysis and Design*, Vol. 11, pp.307-36, 1992.

Mahiou, H., Bekaou, A., "Local stress concentration and the prediction of tensile failure in unidirectional composites", *Composites Science and Technology*, vol. 57, pp.1661–1672, 1997.

Mittelstedt, C., Becker, W., "A single-layer theory approach to stress concentration phenomena in layered plates", *Composites Science and Technology*, vol. 64, pp. 1737–1748, 2004.

Peraire, J., Peiro, J, Formaggia, L., Morgan, K., Zienkiewicz, O.C., "Adaptive remeshing for compressive flow computations", *Journal of Computational Physics*, vol. 72(2), pp. 449-466, 1987.

Peterson, R. E., *Stress Concentration Design Factors*, John Wiley and Sons, New York, 1966.

Pilkey, W.D and Pilkey D.F., *Petreson's stress concentration factors*, John Wiley and Sons, Inc. 3rd edition, January 14, 2008.

Reissner, K., "Transverse bending of plates, including the effect of transverse shear deformation", *Int. J. Solid.y Struct.* vol. 11, pp. 569, 1975.

Savin, G.N., *Stress concentration around holes*, New York, Pergamon Press; 1961.

Ting, K., Chen, K.T., Yang, W. S., "Stress analysis of the multiple circular holes with the rhombic array using alternating method", *International Journal of Pressure Vessels and Piping*, vol. 76, pp. 503–514, 1999.

Toubal, L., Karama, M., Lorrain, B., "Stress concentration in a circular hole in composite plate", *Composite Structures*, vol. 68 pp.31–36, 2005.

Ukadgaonker, V. G. and Rao, D. K. N., "A general solution for stresses around holes in symmetric laminates under in-plane loading," *Composite Structure*, vol. 49, pp. 339-354, 2000.

Ulku babuscu yesil, "The effect of the initial stretching of the rectangular plate with a cylindrical hole on the stress and displacement distributions around the hole", *Turkish J. Eng. Env. Sci.*, vol. 34, pp.1 – 15, 2010.

Watson, David F., "Computing the Delaunay Tesselation with Application to Voroni Polytopes", *The Computer Journal*, vol. 24(2), pp. 167-172 , 1981.

Weatherill, N. P., and Hassan, O., "Efficient Three-Dimensional Delaunay Triangulation with Automatic Point Creation and Imposed Boundary Constraints", *International Journal for Numerical Methods in Engineering*, vol 37, pp. 2005-2039, 1994.

Wu, H., and Mu B., "On stress concentration for isotropic/orthotropic plates and cylinders with a circular holes", *Compos Part B: Eng*, vol. 34(2), pp. 127–34, 2003.

Younis,N. T., "Assembly Stress for the Reduction of Stress Concentration," *Mechanics Research Communications*, Vol. 33, No. 6, pp. 837-845, 2006.

Zhu, J. Z., Zienkiewicz O. C., Hinton, E. and Wu, J. A., "A new approach to the development of automatic quadrilateral mesh generation", *International Journal for Numerical Methods in Engineering*, Vol. 32, pp.849-66, 1991.

Zienkiewicz, O.C., and Taylor, R.L., *The Finite Element Method*, McGraw Hill, London,1989.

APPENDIX

PROGRAM "MESH QUALITY_2012"

```
////////////////////////////////////main.cpp////////////////////////////////////
//quad quality checker for 2d mesh
#include <stdio.h>
#include <stdlib.h>
#include <process.h>
#include "class.h"
#include "function.h"

//Global variables-----
-----
//FILE *fp;//File pointer to inout data
//char inputfilename[256];//

//starting main function

void main(){

    int i, itemp;
    int d1,d2,d3,d4,i2,i3,j,j2,j3,a1,a2,a3,a4,a5,a6,a8;//face number
    double x,y,z,a7;//coordinate of the node on surface mesh
    int numnode,numsurface; //number of nodes and faces of input
    int dummy;
    //char dumy[81], title[81];
    FILE *fp;
    char dumy[81], file1[81];
    puts("Input file name < dr:fn.ext >: ");
    gets(file1);
    fp = fopen(file1, "r");
    //fgets(dumy,80,fp);
    //fgets(dumy,80,fp);
    //fgets(dumy,80,fp);
    //fgets(dumy,80,fp);
    fscanf(fp,"%d %d", &numnode, &numsurface);

    Node*  nodetable[1000];//node information (x,y,z)

    for(i=0;i<numnode;i++){
        fscanf(fp,"%d %lf %lf %lf\n", &itemp, &x, &y, &z);
        nodetable[i] = new Node(x, y, z); //read x,y,z and
store in "coord"
        nodetable[i]->number=i;
    };//end of reading nodedata

    //fgets(dumy,80,fp);
    //fgets(dumy,80,fp);
    //fscanf(fp,"%d", &numsurface);
    //read face data
    //numsurface=numsurface-1;
    Face*  facetable[1000];
```

```

    for(i=0;i<numsurface;i++){
        fscanf(fp,"%d %d %d %d %d\n", &itemp, &d1, &d2, &d3,
&d4);//nodenumbers
        //fscanf(fp,"%d %d %d %d %d\n", &itemp,&d1, &d2, &d3,
&d4);//nodenumbers
        facetable[i]=new Face(nodetable[d1-1], nodetable[d2-1],
                                nodetable[d3-1], nodetable[d4-1]);
        facetable[i]->number=i;
    };//end of reading facedata

fclose(fp); //closing inputfile

Edge*  edgetable[1000];
int numedge=0;

for(i=0; i < numsurface; i++){//loop by number of surfaces
    for(i2=0; i2<4; i2++){
        if(facetable[i]->nextedge[i2] == NULL){
            i3 = (i2<3)?(i2+1) : 0;
            Node* pi1 = facetable[i]-
>node[i2];//no,n1,n2,n3 of a face
            Node* pi2 = facetable[i]-
>node[i3];//n1,n2,n3,no of a face
            //node number of the edge of a surface is
            stored in node[]
            for(j=i+1; j < numsurface; ++j){//betn a face
                and another face
                    for(j2=0; j2<4; j2++){
                        j3 = (j2<3)?(j2+1) : 0;
                        Node* pj1 = facetable[j]-
>node[j2];//
                        Node* pj2 = facetable[j]->node[j3];
                        if((pi1==pj1&&pi2==pj2) ||
(pil==pj2&&pi2==pj1)){
                            edgetable[numedge]=new
Edge(facetable[i],facetable[j],pi1,pi2);
                            edgetable[numedge]->number =
numedge;
                            //---check corner housenn----
                            -----
                            //edgetable[numedge]-
>housenn();
                            Edge* e = edgetable[numedge];
                            facetable[i]-
                            facetable[j]-
                            numedge++;
                            j2=4;
                            j=numsurface;
                        };//if
                    };//for
                };//for
            };//end if nextedge..
        };//end for i2
    }
}

```

```

}; //end for i

//////////quality
program//////////
//flagging the inner nodes (nodes not on boundaries)
for (i=0;i<numedge;i++){
    for(j=0;j<numedge;j++){
        if(j!=i){
            Edge* e0=edgetable[i];
            Edge* e1=edgetable[j];
            if(e0->node[0]==e1->node[0] || e0->node[0]==e1-
>node[1]){
                e0->node[0]->checkn=1;
            }
            if(e0->node[1]==e1->node[0] || e0->node[1]==e1-
>node[1]){
                e0->node[1]->checkn=1;
            }
        }
    }
}
//////////
//Finding neighbor nodes
for(i=0;i<numnode;i++){
    Node* curn=nodetable[i];
    if(curn->checkn==1){
        int h=0;
        for(j=0;j<numedge;j++){
            if(edgetable[j]->node[0]==curn){
                curn->nn[h]=edgetable[j]->node[1];
                h++;
                curn->nnn=h;
            }
            if(edgetable[j]->node[1]==curn){
                curn->nn[h]=edgetable[j]->node[0];
                h++;
                curn->nnn=h;
            }
        }
    }
}

//////////
quadquality(numsurface, facetable);
printquadquality( numsurface, facetable);

}; //end main

void quadquality(int numsurface, Face* facetable[]){
    int i;
    for(i=0;i<numsurface;i++){
        double pi= 3.1415926535;
        if(facetable[i]->number==698){
            int as=2;
        }
    }
}

```

```

        double n010=facetable[i]->node[1]->coord[0]-facetable[i]-
>node[0]->coord[0];//first digit 0=node0, 2nd digit 1=node1, third
digit 0=coord0
        double n011=facetable[i]->node[1]->coord[1]-facetable[i]-
>node[0]->coord[1];
        double n012=facetable[i]->node[1]->coord[2]-facetable[i]-
>node[0]->coord[2];
        double n030=facetable[i]->node[3]->coord[0]-facetable[i]-
>node[0]->coord[0];
        double n031=facetable[i]->node[3]->coord[1]-facetable[i]-
>node[0]->coord[1];
        double n032=facetable[i]->node[3]->coord[2]-facetable[i]-
>node[0]->coord[2];
        double
A=(acos((n010*n030+n011*n031+n012*n032)/(sqrt(n010*n010+n011*n011+n012*
n012)*sqrt(n030*n030+n031*n031+n032*n032)))/pi*180;
        double n100=facetable[i]->node[0]->coord[0]-facetable[i]-
>node[1]->coord[0];
        double n101=facetable[i]->node[0]->coord[1]-facetable[i]-
>node[1]->coord[1];
        double n102=facetable[i]->node[0]->coord[2]-facetable[i]-
>node[1]->coord[2];
        double n120=facetable[i]->node[2]->coord[0]-facetable[i]-
>node[1]->coord[0];
        double n121=facetable[i]->node[2]->coord[1]-facetable[i]-
>node[1]->coord[1];
        double n122=facetable[i]->node[2]->coord[2]-facetable[i]-
>node[1]->coord[2];
        double
B=(acos((n100*n120+n101*n121+n102*n122)/(sqrt(n100*n100+n101*n101+n102*
n102)*sqrt(n120*n120+n121*n121+n122*n122)))/pi*180;
        double n210=facetable[i]->node[1]->coord[0]-facetable[i]-
>node[2]->coord[0];
        double n211=facetable[i]->node[1]->coord[1]-facetable[i]-
>node[2]->coord[1];
        double n212=facetable[i]->node[1]->coord[2]-facetable[i]-
>node[2]->coord[2];
        double n230=facetable[i]->node[3]->coord[0]-facetable[i]-
>node[2]->coord[0];
        double n231=facetable[i]->node[3]->coord[1]-facetable[i]-
>node[2]->coord[1];
        double n232=facetable[i]->node[3]->coord[2]-facetable[i]-
>node[2]->coord[2];
        double
C=(acos((n210*n230+n211*n231+n212*n232)/(sqrt(n210*n210+n211*n211+n212*
n212)*sqrt(n230*n230+n231*n231+n232*n232)))/pi*180;
        double n320=facetable[i]->node[2]->coord[0]-facetable[i]-
>node[3]->coord[0];
        double n321=facetable[i]->node[2]->coord[1]-facetable[i]-
>node[3]->coord[1];
        double n322=facetable[i]->node[2]->coord[2]-facetable[i]-
>node[3]->coord[2];
        double n300=facetable[i]->node[0]->coord[0]-facetable[i]-
>node[3]->coord[0];
        double n301=facetable[i]->node[0]->coord[1]-facetable[i]-
>node[3]->coord[1];

```

```

        double n302=facetable[i]->node[0]->coord[2]-facetable[i]-
>node[3]->coord[2];
        double
D=(acos((n320*n300+n321*n301+n322*n302)/(sqrt(n320*n320+n321*n321+n322*
n322)*sqrt(n300*n300+n301*n301+n302*n302)))/pi*180;
        facetable[i]->df=sqrt(fabs(90-A)*fabs(90-A)+fabs(90-
B)*fabs(90-B)+fabs(90-C)*fabs(90-C)+fabs(90-D)*fabs(90-D));
        facetable[i]->Angle1=A;
        facetable[i]->Angle2=B;
        facetable[i]->Angle3=C;
        facetable[i]->Angle4=D;
        double edl1=sqrt((n010*n010)+(n011*n011)+(n012*n012));
        double edl2=sqrt((n120*n120)+(n121*n121)+(n122*n122));
        double edl3=sqrt((n230*n230)+(n231*n231)+(n232*n232));
        double edl4=sqrt((n300*n300)+(n301*n301)+(n302*n302));
        double biggest, smallest;
        if(edl1>=edl2 && edl1>=edl3 && edl1>=edl4){
            biggest=edl1;
        }
        if(edl2>=edl1 && edl2>=edl3 && edl2>=edl4){
            biggest=edl2;
        }
        if(edl3>=edl1 && edl3>=edl2 && edl3>=edl4){
            biggest=edl3;
        }
        if(edl4>=edl1 && edl4>=edl2 && edl4>=edl3){
            biggest=edl3;
        }
        if(edl1<=edl2 && edl1<=edl3 && edl1<=edl4){
            smallest=edl1;
        }
        if(edl2<=edl1 && edl2<=edl3 && edl2<=edl4){
            smallest=edl2;
        }
        if(edl3<=edl1 && edl3<=edl2 && edl3<=edl4){
            smallest=edl3;
        }
        if(edl4<=edl1 && edl4<=edl2 && edl4<=edl3){
            smallest=edl4;
        }
        facetable[i]->aspr=biggest/smallest;
        int r=3;

        if(facetable[i]->df<=105){
            facetable[i]->pass=1;
        }
        int a=0;
    }
}

void printquadquality( int numsurface,Face* facetable[]){
    FILE* ffile2;
    int i;
    ffile2 = fopen("printquadquality.dat", "w");
    //fprintf(hexfile2,"*****quads with distortion
factor*****\n");

```

```

        fprintf(ffile2,"quad no      angle1      angle2      angle3
angle4      distortion factor  aspect ratio\n");
        for(i=0;i<numsurface;i++){
            fprintf(ffile2,"  %d      %lf      %lf      %lf      %lf
%lf      %lf\n", i+1,facetable[i]->Angle1,facetable[i]->Angle2,
facetable[i]->Angle3, facetable[i]->Angle4, facetable[i]->df,
facetable[i]->aspr);
        }
        fprintf(ffile2,"*****bad quadfaces, distortion factor more
than 105(the passing mark).*****\n");
        for(i=0;i<numsurface;i++){
            if(facetable[i]->pass==0){
                fprintf(ffile2,"%d %lf \n", i+1,facetable[i]->df);
            }
        }
        fprintf(ffile2,"*****average distortion factor and aspect
ratio*****\n");
        double averagedf=0;
        double averagegear=0;
        for(i=0;i<numsurface;i++){
            averagedf=averagedf+facetable[i]->df;
            averagegear=averagegear+facetable[i]->aspr;
        }
        averagedf=averagedf/(numsurface-1);
        averagegear=averagegear/(numsurface-1);
        fprintf(ffile2,"%lf      lf\n", averagedf, averagegear);
        fprintf(ffile2,"*****quad with worst distortion
factor*****\n");
        double worstquad=facetable[0]->df;
        Face* f=facetable[0];
        int numf=f->number;
        for(i=1;i<numsurface;i++){
            if(worstquad>facetable[i]->df){
                worstquad=facetable[i]->df;
                f=f;
                numf=f->number+1;
            }
            if(worstquad<facetable[i]->df){
                worstquad=facetable[i]->df;
                f=facetable[i];
                numf=f->number;
            }
        }
        int a=4;
    }
    fprintf(ffile2," %d, %lf \n", numf, worstquad);
    //////////////////////////////////////
    fprintf(ffile2,"*****quad with worst aspect
ratio*****\n");
    double worstquadar=facetable[0]->aspr;
    f=facetable[0];
    numf=f->number;
    for(i=1;i<numsurface;i++){
        if(worstquadar>facetable[i]->aspr){
            worstquadar=facetable[i]->aspr;
            f=f;
            numf=f->number+1;
        }
    }

```

```
        if(worstquadar<facetable[i]->aspr){
            worstquadar=facetable[i]->aspr;
            f=facetable[i];
            numf=f->number;
        }
        int a=4;
    }
    //////////////////////////////////////
    fprintf(ffile2," %d, %lf \n", numf, worstquadar);
    fclose(ffile2);
};

////////////////////////////////////end main.cpp////////////////////////////////////
```



```

////////////////////////////////////edge.cpp////////////////////////////////////

#include "class.h"
#include "function.h"
Edge::Edge(Face* f1,Face* f2,Node* n1,Node* n2){

    checkflag=0;
    face[0]=f1;
    face[1]=f2;
    node[0]=n1;
    node[1]=n2;

};

////////////////////////////////////end edge.cpp////////////////////////////////////

////////////////////////////////////face.cpp////////////////////////////////////

#include "class.h"
#include "function.h"

Face::Face(Node* d1,Node* d2,Node* d3,Node* d4){
    node[0]=d1;
    node[1]=d2;
    node[2]=d3;
    node[3]=d4;
    nextedge[0]=NULL;
    nextedge[1]=NULL;
    nextedge[2]=NULL;
    nextedge[3]=NULL;
    pass=0;

};

////////////////////////////////////end face.cpp////////////////////////////////////

```

```

////////////////////////////////////class.h////////////////////////////////////

#ifndef class_h
#define class_h

#include <stdio.h>
#include <stdlib.h>
#include <math.h>
#include <time.h>

class Node;
class Face;

class Node {
public:
    int number;//node number
    double coord[3];//coordinate of node

    int checkn;//
    int ev;//edgevalence
    Node* mn[10];//neighbor node
    int nnn;//number of neighbor nodes

    Node(){};

    Node(double x,double y,double z){
        coord[0]=x;
        coord[1]=y;
        coord[2]=z;
        ev=0;
        // checkn=1;
    };//end Node function

};//end class Node
extern int newgennodnum;
extern int gg;

class Edge;
class Face {
public:
    int number;
    int check;
    int checkn;
    double df;//distortion factor for quad quality
    int pass;//1 mean pass, 0 means fail
    Node* node[4];
    Node* nod[18];
    Face* fac[4];
    Face* fa[4];
    double aspr;//aspect ratio

    Face(Node*, Node*, Node*, Node*);//this function has to be
defined outside, in face.cpp

```

```

//as in the function above an outside class is used, so the
function is defined
//in face.cpp
double Angle1;
double Angle2;
double Angle3;
double Angle4;

Edge* nextedge[4];
//Edge* GetOpEdge(Edge*); //for a face, it has two sets of edges.
each set got one edge and the other one is the opedge of the first one

Edge* Find_Common_Edge(Face* next_face){
    Face* f1=this;
    Face* f2=next_face;
    if(f1!=NULL && f2!=NULL){
        for(int i=0;i<4;++i){
            for(int j=0;j<4;++j){
                Edge* e1=f1->nextedge[i];
                Edge* e2=f2->nextedge[j];
                if(e1==e2){
                    return e1;
                } //if e1,e2
            } //for j
        } //for i
    } //if
    return NULL;
} //Find_Common_Edge

};

class Edge {
public:

    int number;
    Face* face[2];
    Node* node[2];
    int checkflag;

    Edge(Face*,Face*,Node*,Node*);

};

#endif

////////////////////////////////////end class.h////////////////////////////////////

```

```
////////////////////////////////function.h////////////////////////////////

#ifndef function_h
#define function_h

//all the functions mentioned any where must be listed here, other
files can get access
//to the functions through this file.
extern Node* newntable[50000];
extern FILE *fp;
extern char inputfilename[256];
void printquadquality( int numsurface,Face* facetable[]);
void quadquality(int numsurface,Face* facetable[]);
#endif

////////////////////////////////end function.h////////////////////////////////
```

EXAMPLE DATA FILE FOR PROGRAM “MESH QUALITY_2012”

27	16				Number of nodes and elements
	1	0.	1.	0.	
	2	0.	5.5	0.	
	3	0.	10.	0.	
	4	.195094	.980785	0.	
	5	1.34756	5.49039	0.	
	6	2.5	10.	0.	
	7	.38269	.923877	0.	
	8	2.69137	5.46194	0.	
	9	5.	10.	0.	
	10	.55558	.831463	0.	
	11	4.02782	5.41573	0.	Node number and coordinates
	12	7.5	10.	0.	
	13	.707107	.707107	0.	
	14	5.35355	5.35355	0.	
	15	10.	10.	0.	
	16	.831472	.555567	0.	
	17	5.41574	4.02777	0.	
	18	10.	7.5	0.	
	19	.923882	.382677	0.	
	20	5.46194	2.69132	0.	
	21	10.	5.	0.	
	22	.980788	.195079	0.	
	23	5.49039	1.34751	0.	
	24	10.	2.5	0.	
	25	1.	0.	0.	
	26	5.5	0.	0.	
	27	10.	0.	0.	
	1	1	2	5	4
	2	2	3	6	5
	3	4	5	8	7
	4	5	6	9	8
	5	7	8	11	10
	6	8	9	12	11
	7	10	11	14	13
	8	11	12	15	14
	9	13	14	17	16
	10	14	15	18	17
	11	16	17	20	19
	12	17	18	21	20
	13	19	20	23	22
	14	20	21	24	23
	15	22	23	26	25
	16	23	24	27	26